OPTIMIZED MITIGATION OF IMPULSIVE NOISE IN OFDM SYSTEM USING CSI

Submitted towards the partial fulfilment of requirement for the award of degree of

Master of Engineering

In

Wireless Communication

Submitted by:

SHIVANI SEHRAWAT

(801463026)

Under the guidance of:

Dr. Amit Kumar Kohli

(Associate Professor, ECED)

ELECTRONICS AND COMMUNICATION ENGINEERING DEPARTMENT

THAPAR UNIVERSITY

(Established under the section 3 of UGC Act, 1956)

PATIALA – 147004, PUNJAB, INDIA

JUNE 2016

DECLARATION

I, **Shivani Sehrawat**, hereby declare that the thesis entitled **"Optimized Mitigation of Impulsive Noise in OFDM System using CSI"** is an authentic record of my own work carried out towards the partial fulfillment for the award of the degree of Master of Engineering in Wireless Communication at Thapar University, Patiala, under the guidance of **Dr. Amit Kumar Kohli**, Associate Professor, Electronics and Communication Engineering Department.

The matter presented in this thesis has not been submitted in any other University/Institute for the award of any other degree.

Date: 30/6/2016

Shivani Sehrawat
Roll No. 801463026

This is to certify that the above statement made by the student is correct to the best of my knowledge and belief.

Date: 30/6/2016

Dr. Amit Kumar Kohli 30/6/2016
Associate Professor, ECED
Thapar University, Patiala

Countersigned by:

(Dr. Sanjay Sharma)
Professor and Head, ECED
Thapar University, Patiala

(Dr. S.S. Bhatia)
Dean of Academic Affairs
Thapar University, Patiala

ACKNOWLEDGEMENT

Foremost, I would like to express my sincere gratitude to my guide **Dr. Amit Kumar Kohli**, Associate Professor and P.G. Coordinator, ECED, Thapar University, Patiala, for his patience, motivation, enthusiasm, immense knowledge and continuous support for my thesis. His guidance helped me in research and writing of this thesis all the time. I would not have imagined having a better guide for my thesis.

Besides my guide, I am thankful to **Dr. Sanjay Sharma**, Professor and Head, Electronics and Communication Engineering Department and **Dr. Hemdutt Joshi**, Assistant Professor, Program Coordinator of Wireless Communication, who have been a constant source of inspiration for me throughout this work, and for providing us with adequate infrastructure in carrying out my work.

I would like to thank all the faculty members of ECED for their full support of my work. I am also thankful to my friends **Sonali, Rohit Garg and Shiv Kumar Sharma**, for encouraging the use of correct grammar and consistent notation in my writings and for carefully reading and commenting on countless revisions of my manuscript. I am also thankful to the authors whose work have been consulted and quoted in this work.

At last but not the least, I would also like to thank my parents for supporting me throughout my life.

Place: Thapar University, Patiala

Date:

Shivani Sehrawat

Roll No.: 801463026

ABSTRACT

Fourth generation (4G) technology aims to provide mobile users with high data rate wireless broadband services with full mobility. Many difficulties are encountered in wireless internet services while providing high speed communication services. These include multipath fading, inter-symbol-interference (ISI) and noise etc. Orthogonal-frequency-division-multiplexing (OFDM) is the technology that provides an effective solution for these problems encountered in high speed wireless transmissions and reception. OFDM has inherent spatial efficiency due to orthogonality between the consecutive subcarriers enabling them to overlap on each other. The use of cyclic prefix enables it to reduce the effects of ISI. Frequency-selective fading experienced in the channel reduces to flat fading in OFDM transmission. Deep fade conditions can hence be observed by limited number of symbols and not by the entire transmission. These advantages have led to replacement of the previously used technologies by OFDM, making it a strong contender for the next generation wireless communication systems.

This thesis presents comparison between different impulsive noise mitigation techniques in orthogonal-frequency-division-multiplexing (OFDM) systems, which affect the performance of underlying communication system in terms of the bit-error-rate (BER). The main focus is on Zhidkov's (ZKV) method (Zhidkov, 2003) and Jia's method (Jia *et al.*, 2014) for the impulsive noise mitigation using the imperfect channel-state-information (CSI). Though former scheme appears to be promising peak detection method based on the variance of estimated impulsive noise, but latter composite-comparison-value (CCV) method is found to be outperforming in alleviating the adverse effects of impulsive noise in the frequency-domain, at the receiving end. In ZKV and CCV methods, different parametric values are optimized to suppress the impulsive noise under the fading conditions in the presence of perfect CSI. Simulation results are presented for performance evaluation of these impulsive noise suppression schemes using imperfect CSI for the different modulation schemes, which illustrate the efficacy of CCV method in the field of communication engineering.

Keywords: OFDM, impulse noise, channel estimation, channel state information, DFT, IDFT

TABLE OF CONTENTS

LIST OF ACRONYMS AND ABBREVIATIONS

4G	Fourth Generation
A/D	Analog to Digital
AGC	Automatic Gain Control
AWGN	Additive White Gaussian Noise
BER	Bit Error Rate
CCV	Composite Comparison Value
CP	Cyclic Prefix
CSI	Channel State Information
D/A	Digital to Analog
DAB	Digital Audio Broadcasting
DFT	Discrete Fourier Transform
DSL	Digital Subscriber Line
DVB	Digital Video Broadcasting
DVB-T	Terrestrial Digital Video Broadcast
FDM	Frequency Division Multiplexing
FFT	Fast Fourier Transform
I/P	Input
ICI	Inter-Carrier Interference
IDFT	Inverse Discrete Fourier Transform
IEEE	Institute of Electrical and Electronics Engineer
IFFT	Inverse Fast Fourier Transform
IIR	Infinite Impulse Response
ISI	Inter-Symbol Interference
LOS	Line of Sight
MATLAB	Matrix Laboratory
MCM	Multi-carrier Modulation
O/P	Output
OFDM	Orthogonal Frequency Division Multiplexing
OFDMA	Orthogonal Frequency Division Multiple Access
PAPR	Peak-to-Average Power Ratio

PDF	Probability Density Function
PLC	Power Line Communication
PSK	Phase Shift Keying
QAM	Quadrature Amplitude Multiplexing
QoS	Quality of Service
QPSK	Quadrature Phase Shift Keying
RMS	Root Mean Square
RS	Reed Solomon
SER	Symbol Error Rate
SNR	Signal-to-Noise Ratio
WDM	Wavelength Division Multiplexing
Wi-MAX	Worldwide Interoperability for Microwave Access
WLAN	Wireless Local Area Network
ZKV	Zhidkov

LIST OF FIGURES

LIST OF TABLES

Chapter 1

INTRODUCTION

This chapter introduces the thesis work. This brief introduction includes orthogonal-frequency-division-multiplexing (OFDM), its comparison with other single-carrier and multi-carrier schemes and impulsive noise. This chapter concludes with the details about the organization of the thesis.

1.1 Introduction

The last couple of decades have seen an exponential growth in the communication sector. With this growth, the demand for a high speed and noise resistant communication system has also increased. Coupled with the limited bandwidth available for communication, the advancements have shifted from a single-carrier communication system to a multi-carrier communication system [1].

A single-carrier communication system suffers from inter-symbol-interference (ISI), and to avoid this problem the duration of the symbol period should be much greater than the delay time. This long symbol period leads to lower data rate, as symbol period is inversely proportional to data rate. This leads to inefficiency in the communication system. In the case of multi-carrier communication systems, such as frequency-division-multiplexing (FDM), the total available bandwidth, in the spectrum, is divided into small sub-bands for different carriers to transmit in parallel. When these carriers are placed very close to one another in the spectrum, the overall data rate achieved by the system improves significantly. However, when the spacing between the carriers is less, the system suffers from inter-carrier-interference (ICI) [1]-[2]. To avoid the condition of ICI, guard bands are needed to be placed in between consecutive carriers, but these guard bands result in reduction in the useful bandwidth that can be used for data transmission [2].

Orthogonal-frequency-division-multiplexing (OFDM) is a type of multi-carrier transmission technique that solves both issues and is being widely used in the 4^{th} generation wireless communication systems. It works with a composite high data rate communication system that is essentially a combination of many low data rate subcarriers. The property of orthogonality, in the OFDM system, enables the carriers to be closely spaced, even

overlapped, without causing ICI. Each individual carrier has low data transmission rate, so this implies long symbol periods, which reduces the effects of ISI [3].

OFDM is popularly used in both wired as well as wireless broadband communication systems because it solves the problem of ISI. This is important when the data rates increase and the received signal starts to depend on a number of consecutive transmitted symbols. Another noteworthy advantage of OFDM is its capability to transfer the complexity of transmitters and receivers from the analog to the digital domain. In OFDM systems, the phase variation with frequency is corrected at minimum cost in the digital part of the receiver [4].

Despite the similarities between OFDM systems and conventional multi-carrier communication systems, there are many differences. The subcarrier frequencies, in OFDM, are chosen in a way to ensure that orthogonality is achieved in the signals mathematically over each OFDM symbol. Both modulation and multiplexing operations are achieved by inverse-discrete-Fourier-transform (IDFT). This results in the required precision in orthogonality of the signals in a very computationally efficient way. In FDM and wavelength-division-multiplexing (WDM), we use frequency guard bands between the subcarriers [4].

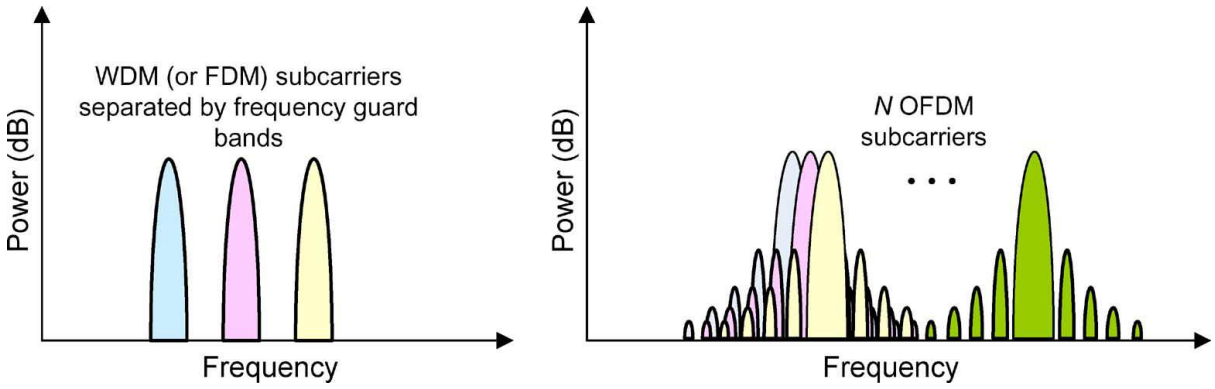

Fig. 1.1. Spectral representation for (a) WDM and/or FDM signals (b) OFDM signal [4].

As shown in the Fig. 1.1, the spectrum of OFDM differs from the spectrum of FDM/WDM as the individual subcarriers overlap with each other. Because of orthogonality between consecutive subcarriers, the demodulation and demultiplexing of the received subcarriers can be done without interference subjected to the condition of linearity of the channel. The discrete-Fourier-transform (DFT) is performed at the receiver for demodulation and demultiplexing. Each subcarrier in OFDM can be spectrally represented by the form $\left|\sin(x)/x\right|^2$. This results in significant side lobes of each subcarrier in the frequency range [4]. This causes sensitivity to frequency-offset and phase noise in OFDM system [1]-[2], [4].

Alongside these factors, the OFDM system is also affected by the noise present in the channel. This includes the additive-white-Gaussian-noise (AWGN) and impulse noise. Impulse noise is characterized by high amplitude and short duration that is caused by the power lines, high power switches, sharp sounds, ignition system etc. [5]-[6]. The varied range of sources for the impulse noise results in a number of approximate models including but not limited to Poisson-Gaussian model, Bernoulli-Gaussian model [7]-[10]. Another modeling technique that is popularly used for realistic approximation of impulsive noise is gated Gaussian modeling [11]-[13]. Impulsive noise overloads the amplifiers at the receiver end and also affects the automatic-gain-control (AGC) due to its high power [4]. The noise bucket effect effectively reduces the impact of impulse noise in OFDM system; but in case of high amplitude impulse noise, this becomes a disadvantage. Instead of reducing the effect, the system performance further deteriorates [12].

Impulsive noise needs to be removed from the received signal before the signal can be processed for information. Many approaches have been proposed over the time for mitigating the effects of impulsive noise from the received signal. The simplest approach is clipping. The part of the received signal that exceeds the threshold is considered to be part of impulsive noise, and hence clipped [9], [11], [13]. Another method that is used is blanking nonlinearity. It is similar to clipping, but the signal that exceeds the threshold is replaced by a zero [5], [8], [14], [15]. Both these methods are time-domain impulsive noise suppression method. This work discusses two methods employed in frequency-domain. First method is proposed by Zhidkov [14]. This method (ZKV method) is a variance based peak detection method. The second method, proposed by Jia and Meng [15] is a modified mean replacement method that calculates composite-comparison-value (CCV) for determining the impulsive noise and then removes it from the received signal [15]. The performances of both these techniques are analyzed under different conditions, and the parameters used in these systems are optimized under the perfect channel-state-information (CSI). Further, these methods are studied for imperfect CSI using the approach proposed by authors in [16]. The results present the bit-error-rate (BER) performance of these systems under different the simulation conditions.

1.2 Motivation

Latest communication systems demand for high data rate along with high noise immunity [5]. This has led to a shift in focus from the conventional single-carrier modulation schemes to multi-carrier modulation schemes [4]. Orthogonal-frequency-division-multiplexing (OFDM)

is a multi-carrier modulation (MCM) scheme based on inverse-discrete-Fourier-transform/ discrete-Fourier-transform (IDFT/DFT). It has found applications in wired as well as wireless based communication systems including optical systems, digital-audio-broadcasting (DAB), digital-video-broadcasting (DVB), wireless-local-area-networks (WLAN), power-line-communication (PLC) etc. [4], [15]. This is due to the improved noise immunity provided by an OFDM system because the noise (thermal and man-made) interferes with the time-domain signal, and gets spread over the entire symbol period in frequency-domain. This innate noise immunity along with the low complexity compensation methods for the noise reduction has improved quality-of-service (QoS) for OFDM system even under the highly noisy environments [5].

The high amplitude and small duration man-made noises in the environment contribute to generate the impulsive noise. Sources of impulsive noise are vehicular ignition systems, electrical appliances, power lines, high power switches etc. [8]. The effects of impulsive noise are severe on the performance of receiver, as it overloads the input amplifier and disrupts the automatic-gain-control (AGC) due to its high power [12]. As a remedial solution, the limiting nonlinearity is a simple and basic scheme used to suppress impulsive noise. Another strategy popularly used in practical systems is the blanking nonlinearity technique. Both these schemes are used to process received signal in time-domain to replace the samples of signals, which are above a predetermined threshold value [9]. Although it has been extensively utilized in realistic OFDM systems to combat impulsive noise, yet it reduces signal power and also generates inter-carrier-interference (ICI) [5]. Zhidkov has proposed ZKV method in [14], which uses the frequency-domain equalization followed by the estimation of impulsive noise using the variance of estimated noise. Another type of method, that is commonly used, is the conventional mean filter [15]. In this method, the output of filtering process is a rough approximation of the original transmitted signal. Though the signal is poorly represented, but gain is achieved at the receiver by removing impulsive noise [15]. Jia and Meng have proposed the composite-comparison-value (CCV) method in [15], which outperforms mean replacement scheme. A modified mean filtering strategy is used in this scheme to detect the impulsive noise present in the received signal, and it effectively extracts the desired transmitted signal.

In this research work, we compare the results obtained by applying ZKV scheme [14] and CCV scheme [15] for impulsive noise mitigation in the OFDM system. The parameters, which need to be optimized, are the threshold value for ZKV scheme and window size for CCV scheme using the perfect channel-state-information (CSI). Further, the imperfect CSI

scenario is discussed for these schemes to observe their effectiveness while using different modulation schemes under different impulsive noise conditions. The presented work is an extension of the results and observations proposed in [16].

1.3 Thesis Objective

This thesis is an attempt to understand and analyze different methods used for the impulsive noise mitigation in the OFDM system and also to obtain optimized parameters used in these methods under different conditions/ specifications. OFDM system under fading environment, which is corrupted by AWGN and impulsive noise in the channel can be described as

$$r_m = x_m * h_m + w_m + i_m \tag{1.1}$$

In this system, h_m is the channel characteristic, w_m is the AWGN and i_m is the impulsive noise. i_m is modeled using gated Gaussian modeling. Here, * is the linear convolution operator. At the receiver, the impulsive noise is mitigated using two different approaches: Variance based peak detection method (ZKV) and composite-comparison-value (CCV) method. The parameters used in these methods are varied and then optimized to understand their effects on the performance of the system under simulation. To obtain a realistic understanding of the underlying OFDM system with impulsive noise mitigation techniques, it has been further analyzed under imperfect channel-state-information (CSI) environment.

1.4 Organization of Thesis

The remaining thesis is organised as

- **Chapter 2: Literature Survey:** In this chapter, the literature survey for mitigating the effects of impulsive noise is discussed.
- **Chapter 3: Fundamentals of Orthogonal Frequency Division Multiplexing:** This chapter discusses the OFDM system, its block diagram, mathematical model and the implementation of the system using MATLAB.
- **Chapter 4: Impulsive Noise Mitigation Techniques Under Fading Environment:** This chapter discusses the different types of fading caused in the channel. The impulsive noise and its modelling have been discussed. This chapter provides the details of the impulsive noise mitigation schemes used in the OFDM system.

- **Chapter 5: Optimization of the Parameters for Impulsive Noise Mitigation Methods:** Mathematical analysis of imperfect CSI and the OFDM system under impulsive noise environment have been presented. Further the simulation results for optimization of the parameters used in these methods have been discussed under perfect CSI and imperfect CSI.
- **Chapter 6: Concluding Remarks and Future Scope:** In this last chapter, the thesis work has been concluded by discussing the performance of the three systems under different simulation conditions for perfect CSI and imperfect CSI. Some ideas for future research work have been suggested.

Chapter 2

LITERATURE SURVEY

This chapter provides survey of the severe effects of the impulsive noise on the OFDM system and the techniques available in literature for impulsive noise mitigation.

Effects of Impulsive Noise and its Suppression in OFDM System

In [5], Yih discusses a modified form of blanking nonlinearity method for the impulsive noise mitigation. The blanking nonlinearity method is the most simple and is used practically in OFDM system for the cancellation of the effects of impulse noise. Blanking nonlinearity is a nonlinear operation, so it disturbs the orthogonality of the OFDM system and hence causes ICI. The proposed method helps improving the performance by detecting and reducing the effects of ICI, impulse noise and the ICI caused by nonlinear blanking method. The performance of OFDM system is improved by iteratively increasing the value of threshold value. If the value of threshold is fixed, the results converge for greater number of iteration. But with adaptive value of threshold, the number of iterations reduces. Initially the optimum value of threshold is calculated and it is kept fixed to reduce computational complexity. But, this value may not be optimum value for successive iterations. This causes results to converge in greater number of iterations. But, if the value of threshold is iteratively increasing, the results converge with lesser number of iterations but at the cost of increased computational complexity.

In [8], Zhidkov has discussed the blanking nonlinearity method for the impulsive noise cancellation. Blanking nonlinearity is one of the simpler methods for excision of impulsive noise, and is used in time-domain mitigation of impulsive noise. The threshold value for blanking the OFDM signal corrupted by impulsive noise has been calculated theoretically under different scenarios of impulsive noise models. The only assumption for the method analyzed and presented is that the number of OFDM subcarriers is large. When using only this assumption, the analysis can be validated for other communication signals that are using complex Gaussian modeling. The impulsive noise model used for analysis is a mixture-Gaussian model, and this enables the analysis to be extended to non-Gaussian modeling as

well. The author also presented a closed form expression at the output of the blanking nonlinearity for signal-to-noise ratio (SNR). This SNR is then maximized for optimal threshold used for blanking nonlinearity.

Mengi and Vink [9] have proposed a method for convergence of the OFDM system performance when the number of subcarriers is greater than or equal to 64 in a symbol period. The technique is applied to the narrowband power line communication system, which is high data rate application working on 500 kHz range. In this range, the channel is highly corrupted by high amplitude impulsive noise and short duration. And since the channel used is narrowband, the number of subcarriers is less, and hence the impulsive noise makes the channel unusable. To reduce the effect of this impulsive noise on systems using less number of subcarriers, the authors have proposed the usage of clipping and nulling iteratively for convergence of results even in cases with number of subcarriers as low as 64. For higher number of subcarriers, this technique leads to fast convergence of the system performance. The authors have further proposed a novel technique using low complexity syndrome decoder for synchronization; and other purposes by using redundancies. The results have been presented showing an improvement in performance of the system while using this technique.

In [10], Ghosh has explained the effects of impulsive noise on multi-carrier systems and also on single-carrier systems. Both these systems have their performance severely affected by the probability of occurrence of impulsive noise. The model for impulsive noise is said to be defined as a product of two processes: one is real Bernoulli process and the other is complex Gaussian process. This is thought of as though the transmitted signal is affected by impulsive noise with Gaussian characteristics with probability of occurrence equal to p. The paper simulated the OFDM system affected by Bernoulli-Gaussian model for impulsive noise under quadrature-amplitude-modulation (QAM) modulation scheme. Author further provided simulation results for performance of multi-carrier system and single-carrier system under different probabilities of impulsive noise occurrences. From the results, it is inferred that the performance of multi-carrier system is better than to single-carrier systems when the probability of the impulsive noise is low. But the single-carrier system perform better when the probability of the impulsive noise is increased.

In [11], Suraweera *et al*. discusses the effects of impulsive noise on OFDM system. It also explains the spreading effect caused in OFDM system because the DFT block at the receiver results in the spreading of noise power in the entire symbol period. Thus, reducing its impact

on individual subcarrier and also reducing the peaks that may affect other components of the receiver like the AGC. Further, it also discusses the models that can be used for impulsive noise. The most suitable model for digital television system is the gated Gaussian model, in which the noise can be explained as sum of AWGN for the symbol duration T and Gaussian impulse noise for a fraction of symbol period. It also discusses mitigation techniques that are commonly used: nulling vs. clipping. If the noise sample is known correctly, nulling is the preferred choice but it causes distortion in the signal in case the noise is incorrectly identified. The signal received is checked against a threshold measure. The signal is passed on to the demodulator if its level is lower than the level of threshold level. The signal is nulled if its level crosses beyond the level of threshold. The high level peaks are considered to be impulsive noise and hence ignored. This blanking method is nonlinear and hence Bussgang's theorem is used for analysis.

Suraweera and Armstrong [12] have discussed the noise bucket effect observed in the OFDM systems. Impulsive noise is citied as a major performance degradation factor in these systems. This paper discusses the degradation in performance of OFDM system when affected by impulsive noise, and its dependence on the total energy of the impulsive noise in one symbol period. For small number of impulses in the OFDM symbol, the distribution of the noise component at the receiver can be said to be Gaussian. This is not dependent on the nature and structure of individual impulsive noise component. The BER in case of impulse noise is seen to be same as the BER of the system affected by Gaussian noise for total noise per symbol. Noise bucket effect is defined as the spreading of the noise energy in the entire symbol period at the receiver after passing through the fast-Fourier-transform (FFT) block. This results in the degradation of the system performance depending on the total energy of impulsive noise in the symbol period of OFDM system instead of the structure of impulsive noise.

In [13], Armstrong and Suraweera have proposed a new method for estimation, and hence the suppression of impulsive noise in OFDM system. Pilot tones are not used in this new technique for the estimation of the impulsive noise. The estimation of the impulsive noise is done for each received signal sample. The value of the received component sample is subtracted from the estimated noise component if the value of the received sample is large. The estimated noise signal is obtained by preliminary decision of the noisy signal. The noise power is greatly reduced in case of system affected by impulsive noise. This method is also

nonlinear in nature, and hence Bussgang's theorem is used for decision process. The improvement in the BER when using this technique is of the order two to three in magnitudes.

Zhikov [14] has proposed a new frequency-domain algorithm for mitigation of impulsive noise in the OFDM based systems. The advantage of spreading in long duration OFDM symbol period is used when the impulsive noise has low amplitude. This enables the energy of the impulsive noise to spread across the entire symbol. If the impulsive energy is low, it provides an advantage but it drastically reduces the system performance if the energy of the impulsive noise is high. The method proposed in this paper, called as impulsive noise compensation method, is used in frequency-domain and hence applied after the OFDM demodulation and channel equalisation. This is opposed to other methods for suppression of impulsive noise that are applied to the received signal before demodulation and equalisation. The author presents simulation results of this method under 64-QAM modulation scheme and using Bernoulli-Gaussian model for impulsive noise. This method can be used in terrestrial digital video broadcast (DVB-T) systems, which have serious performance degradation due to impulsive noise.

Jia and Meng [15] have proposed a two stage scheme for suppressing the impulsive noise by using a modified mean filter and Reed-Solomon (RS) coding for detecting and removing impulsive noise that may cause bursty noise in the OFDM symbol. The novel mean filtering technique using composite-comparison-value (CCV) is proposed by the authors that effectively suppresses the impulsive noise. In this scheme, the received signal is equalized and then sampled for the purpose of evaluating the CCV for the sampled signal train and also the original signal train. The comparison of these sampled signals helps in detecting the impulsive noise. To make the scheme more robust, RS codes are used. The usage of RS codes after effectively removing the impulsive noise makes the determination of the original signal more accurate. Also, in case of any residual impulsive noise, the second stage of RS codes is useful. The performance of this dual-scheme has been analysed and presented in this paper is compared with the results when only a single stage filtering and when coding techniques is used.

Bansal *et al.*, in [16], have discussed OFDM with impulsive noise suppression scheme for the Nakagami-m multipath fading channel. Further, due to the inevitability of error introduced by the imperfect channel estimation process at the receiver, the underlying system has been

studied for the imperfect CSI. The impulsive noise suppression is done using blanking nonlinearity. This scheme uses frequency-domain detection and suppression of impulsive noise. The authors have used Bernoulli-Gaussian model for modelling the impulsive noise. This model assumes that impulsive noise can be modelled as the product of two independent variables, one of them Bernoulli and the other complex Gaussian. The channel estimator has a major role in the performance of the system because the errors in estimation process can severely degrade the performance of the system. The results are also discussed to observe the effects of changing value of m for the Nakagami-m multipath fading on the BER performance of the underlying system. When the scheme proposed in this paper is applied iteratively, the performance of the system supersedes the performance of single iteration system and even the system using blanking nonlinearity under the underlying condition of low estimation errors in the channel estimation process.

Abdelkefi *et al*., in [17], have described a procedure for cancellation of impulsive noise using syndromes that are scattered in the transmitted symbols. The transmitted signal in the channel is corrupted by different types of noise including impulsive noise and AWGN. A channel decoding type procedure is used on the received signal to remove the impulsive noise from it. The signal has syndromes spread in it among the information bits along with pilot tones. The pilot tones perform the task of synchronization of symbols and also for estimation purposes. Both these types of symbols are sent among the information bits to help the receiver estimate and detect; and hence cancel the effects of the noise from the useful bits. A powerful encoder is employed at the receiver for this purpose. This encoder is called the Reed-Solomon (RS) encoder. Impulsive noise cancellation is accomplished by this encoder. The received signal vector of each component is used to cancel the impulsive noise. The total number of impulses and the location of each impulsive noise component are found using singular value decomposition.

Al-Naffouri *et al*., in [18], have proposed a new scheme for cancelling the effects of impulsive noise using reconstruction of sparse signals that are observed through projections. The proposed method uses convex programming techniques and also compressed sampling. This method increases the robustness of the system against the background noise added in the channel. For an OFDM system affected by severe fading, some frequencies are greatly attenuated. These frequencies may have either information bits or pilot tones. This may lead to loss of data or can compromise the synchronization and estimation done at the receiver. In

case pilot tones are affected, this method proposes to reconstruct the projection matrices. The BER is then compared for a method using upper or lower bounds with a capacity for a Gaussian erasure channel. The proposed method cannot locate the positions of the impulsive noise, but can cancel its effects on the OFDM system.

In [19], Chen *et al*. have proposed a new low complexity technique that aims to estimate and compensate the effects of impulsive noise in orthogonal-frequency-division-multiple-access (OFDMA) systems. In the other methods that are available for impulsive noise compensations, the receiver needs all the demodulated symbols for clipping the noise component. But in the proposed method, the receiver need not know all the modulated symbols. The technique used in this paper has utilized the equalised output to detect the number of clippings done; and by using this information on the subcarriers that are known, it reconstructs the clipping signal. This method is particularly useful in cases when the user does not have complete knowledge of the entire signal and has to work with limited knowledge. In OFDMA systems, the knowledge of the clipping noise is used for the recovery of the transmitted signal. The information of the known subcarriers is used for signal recovery instead of the conventional direct decision directed approach. This method has found application in worldwide-interoperability-for-microwave-access (Wi-MAX) systems where a small percentage of the subcarriers is known to the receiver. The equalised signal is used to obtain the locations of the clipped signal using the known subcarriers. This is then fed to the equation for determining the clipped noise. The paper also presents the simulation results which show that the system performance can be improved significantly when using this method.

Kitamura *et al*., in [20], have proposed a scheme, which uses iteration for suppression of the impulsive noise. Impulsive noise has small duration and wide frequency band. In DFT-based systems, the energy of the impulsive noise spreads to the entire symbol and with high probability of the impulsive noise, all the symbols are affected. This degrades the performance of the system severely. In cases with high amplitude impulsive noise, the subcarriers are also affected severely. In the proposed method, during each iteration, the replicated signal is subtracted from the corrupted received signal to mitigate the effects of the impulsive noise. The process is done in the time-domain by iteratively subtracting the estimated signal from the received signal. This proposed method can be explained as: the received signal corrupted by impulsive noise is first passed through the DFT block to

demodulate the signal. Equalisation is then performed on this signal for estimation of the noise. Channel characteristics are then multiplied to the symbols. After performing IDFT on this signal, it is subtracted from the received signal. The output is the noise signal. This process is done iteratively to improve system performance.

In [21], Lampe has proposed a scheme for reducing the effects of impulsive noise occurring in bursts. For this scheme, the author has assumed that the duration of bursts is smaller than the coding frame for successful mitigation of the impulsive noise. The method is based on compressed block sensing. This scheme is particularly used in the PLC systems using OFDM transmission. The system uses null subcarriers to detect the structure of the impulsive noise and determine the location and the magnitude of the bursts of noise samples. For proper determination of the noise, the length of OFDM symbol must be greater than the length of burst noise. If the length is smaller than the burst noise, then the entire symbol is lost and cannot be recovered. The bursts of the impulsive noise is said to be based on the compressed sensing technique of the block sparse signals. This application of compressed sensing technique can successfully cancel the effects of impulsive noise of bursty nature and greatly improve the reliability of transmission under these conditions. Numerical results have been found, based on compressed sensing technique, which can estimate the bursts of impulsive noise and help improve system performance.

In [22], Al-Naffouri *et al*. have proposed a scheme that relies on guard band subcarriers for both the functions of estimation and mitigation of impulsive noise. Impulsive noise is a major deterrent to the performance of OFDM in digital-subscriber-line (DSL) communication. In the proposed method, impulsive noise is taken as a sparse vector; and the sparse reconstruction algorithm is used to mitigate the impulsive noise. *A priori* information is used for the sparse signal recovery algorithm. The complexity of the sparse reconstruction algorithm is lower than the other conventional mitigation techniques available. The null subcarriers of the guard band are used for the process of estimation, and hence the cancellation of the impulsive noise is performed. Bayesian method is used in the compressed sensing procedure. This will provide the *a priori* information needed for the estimation process with reduced complexity. The system using this technique provides a better performance as compared to other conventional techniques available including other sparse recovery techniques and the minimization techniques. The proposed method also achieves a higher data rates needed in the DSL communication lines.

Tseng *et al.*, in [23], have proposed a new method for the mitigation of impulsive noise without using *a priori* knowledge. The value for threshold used for clipping is derived without *a priori* information regarding the probability-density-function (PDF) of the impulsive noise. This is important in the practical scenarios as the PDF of the impulsive noise changes rapidly with time. The clipping in this method utilises decoding matric. The method losses its effectiveness, when the probability of the impulsive noise increases. In this case, the clipping threshold increases the BER drastically, when the clipper is placed ahead of the demodulator.

In [24], Ren *et al.* have proposed a scheme for reducing the severity of the impulsive noise by using infinite-impulse-response (IIR) notch filters. The signal, which is received at the receiver, is the result of the interference between the transmitted signal and the periodic impulses in the channel. This is equivalent to the addition of damping sinusoids to the signal. The occurrence of the impulsive noise in the channel affects the synchronization of OFDM and the PLC system. The system performance gets degraded and its working is affected. The impulsive noise, thus, need to be suppressed from the received signal to improve synchronisation and performance of the underlying system. This also removes the degrading effects of impulsive noise from the received signal. To remove the impulsive noise, the proposed method follows the following three steps: first step is to detect and estimate the impulsive noise along with its location in the received signal, the second step is to determine the frequency of occurrence of the impulsive noise and the final step in the proposed algorithm is to remove the estimated impulsive noise using an adaptive IIR filter. The output of the IIR filter is the desired signal without the impulsive noise component. This proposed method is suitable for narrowband applications.

In [25], Mathew and Jeevitha have proposed two algorithms for reducing the effects of impulsive noise from the received signal. The duration of the OFDM symbol can be assumed to be much longer than the duration of the impulsive noise. When the strength of impulsive is less, the spreading effect on the long OFDM symbol provides immunity against this weak impulsive noise. The spreading effect of the FFT operation at the receiver leads to the impulsive noise affecting all the subcarriers in the OFDM symbol. The two algorithms proposed by the authors are for locating the impulsive noise in the received signal and for determining the value of the impulsive noise. This helps in estimating the impulsive noise. The estimated impulsive noise can then be removed from the received signal. This improves

the system performance significantly. This proposed scheme can also be applied iteratively to further reduce the degrading effects of the impulsive noise, and further improve the performance of the OFDM system significantly.

Chapter 3

THEORY AND CONCEPTS OF OFDM

This chapter presents an introduction to the OFDM system. It also discusses the mathematical model for OFDM system along with the block diagram. The effects of AWGN and distortions in the channel are also studied. It also presents the implementation and simulation of the OFDM system using MATLAB for understanding the effects of modulation techniques, number of subcarriers and the fading conditions on the performance of the OFDM system. The advantages and disadvantages are discussed towards the end of the chapter.

3.1 Introduction

In the past few years, wireless technology has experienced an explosion in terms of growth. This growth has opened new avenues in the wireless communication field with the ultimate goal to unify the personal as well as multiuser communication with minimal to zero regard to location or mobility of the user and also providing connectivity at high data rates. This new objective of the communication networks support the high transmission rate applications and services like high-quality videos, live streaming, and mobile integrated digital service network. When the data transmission takes place at such high bit-rates, the impulse response of the channel extends over many symbol periods, leading to ISI. OFDM has emerged as a new candidate for mitigating ISI. The bandwidth is divided into narrow subchannels which are then used to transmit data in parallel at lower data rates. As the data rate is lower, the symbol-period is longer and hence ISI affects one symbol period at most. The subchannels are chosen to be narrow enough to eliminate the effects of delay spread in the channel.

3.2 Basic Concepts of OFDM

3.2.1 Orthogonal Frequency Division Multiplexing

Orthogonal-frequency-division-multiplexing (OFDM) is based on the worldwide interoperability for microwave access [1]. It supports high data rates of about 100 Mbps, which is widely used in the wireless broadband technology. It also presents an effective solution to reduce the effects of ISI, which is caused in dispersive environment. It is also resistant to the multipath fading [4].

OFDM is a multi-carrier modulation (MCM) scheme [26]. The transmission in this scheme takes place by breaking the available bandwidth into N subchannels. Each of these subchannels is a smaller band with bandwidth smaller than the single-carrier modulation systems [26]. This provides OFDM systems robustness against the frequency-selective fading, as the bands are small and the frequency-selective fading reduces to flat fading for individual bands. In conditions with deep fading, the entire link is compromised for the single-carrier systems. But in case of OFDM system, only a selective few subcarriers are affected [27], [28].

The data is now transmitted over these subcarriers in parallel on different frequencies. This leads to longer length of the symbol period as compared to the single-carrier systems. If the data rate is kept constant for both the systems then the symbol time can be compared as:

For single-carrier systems, the symbol time can be expressed as

$$T = \frac{1}{B} \tag{3.1}$$

For multi-carrier systems, the symbol time can be expressed as

$$T = \frac{N}{B} \tag{3.2}$$

where, B is the symbol rate that is kept constant for the two systems, N is the number of subcarrier frequencies used in the multi-carrier system. In OFDM systems, these N frequencies are chosen such that they are orthogonal, hence overlapping, to each other. This overlapping of subcarrier channels saves 50% bandwidth as the guard band is now added between the symbols and not between all the multiple frequencies as in the case of FDM [1]. It has been shown in Fig. 3.1.

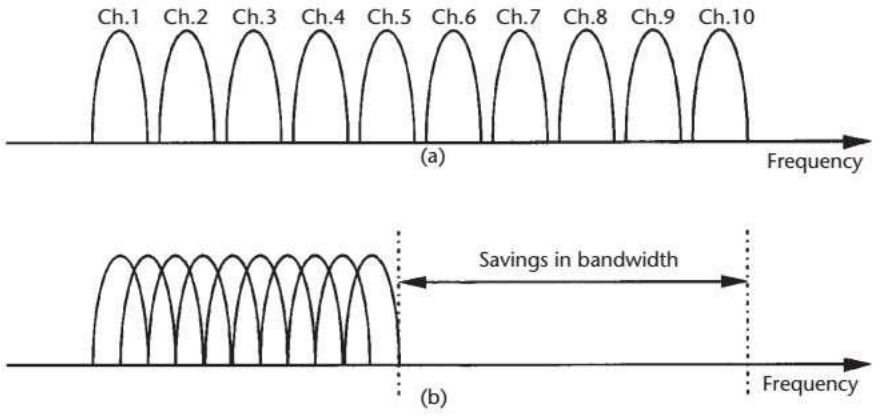

Fig. 3.1. Bandwidth use in different multi-carrier systems (a) FDM system and (b) OFDM system [1].

3.2.2 Generation of OFDM Signal for Transmission

The digitalized data to be transmitted is first modulated using different modulation schemes like quadrature-amplitude-modulation (QAM) or phase-shift-keying (PSK). This complex symbol stream is then converted to parallel blocks of size N symbols each to be fed into the IDFT, where N is the number of subcarriers. The output of the IDFT is then appended with cyclic prefix to improve system performance against ISI. DFT is used at the receiver end to perform the reverse action of IDFT at transmitter. Practically, the function of IDFT/DFT is performed by inverse-fast-Fourier-transform (IFFT) at the transmitter end and by fast-Fourier-transform (FFT) at the receiver end.

3.3 Mathematical Model

The main distinguishable function in OFDM system is performed by the IFFT/FFT blocks. IFFT is used at the transmitter end to perform multiplexing and modulation. The corresponding function of demodulation and demultiplexing is done by FFT block at the receiver end [4]. The orthogonality of the subcarriers and the spacing between the subcarriers is also defined by using these blocks. The OFDM system is described by the block diagram in Fig. 3.2.

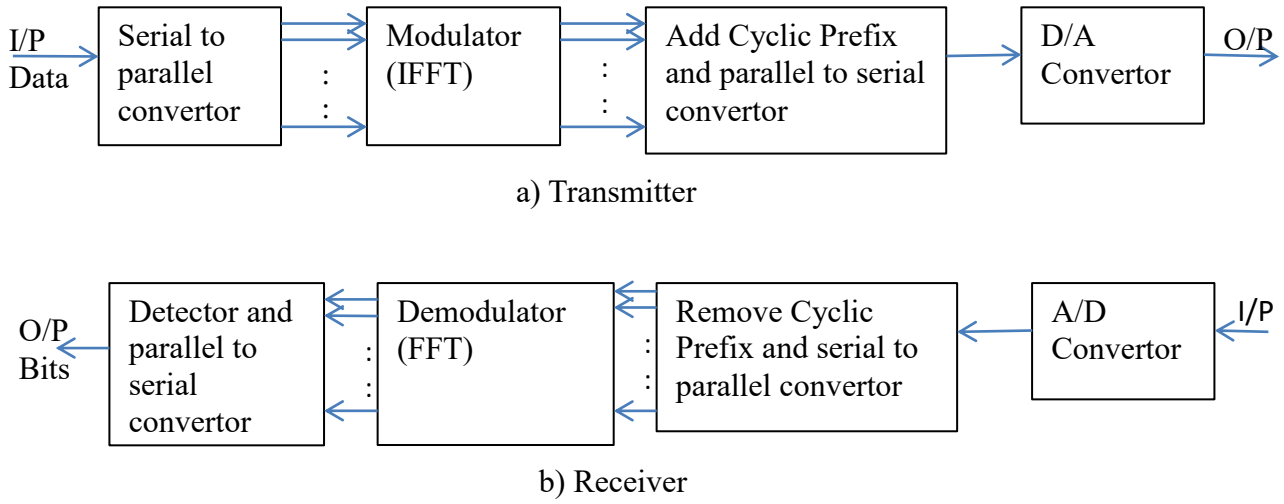

Fig. 3.2. Block diagram for OFDM system.

IFFT takes in the input as a complex vector $X = \left[X_0\ X_1\ X_2 \cdots X_{N-1}\right]^T$ that has the length N; where N is the symbol size of the IFFT [29]. All the elements of input vector represent the data, that is to be carried on the corresponding subcarrier. Therefore, X_k represents the data to be carried on the k^{th} subcarrier. QAM modulation scheme is usually used in OFDM, such

that each element is a complex number represented as a particular constellation point of QAM [4].

The IFFT output is also a complex vector. According to the definition, used in this work, of the inverse-discrete-Fourier-transform, the output is obtained as

$$x_m = \frac{1}{\sqrt{N}} \sum_{k=0}^{N-1} X_k \exp\left(\frac{j2\pi km}{N} \right) \qquad for\ 0 \le m \le N-1 \tag{3.3}$$

The pair of forward and inverse-fast-Fourier-transforms used in this text are defined in slightly differently way. The forward FFT corresponding to above IFFT of Eq. (3.3) is:

$$X_k = \frac{1}{\sqrt{N}} \sum_{m=0}^{N-1} x_m \exp\left(\frac{-j2\pi km}{N} \right) \qquad for\ 0 \le k \le N-1 \tag{3.4}$$

This form of the IFFT/FFT pair used in this work offers the advantage that the discrete signals at the input and the output for each symbol has the same total energy and the same average power. This simplifies the calculations of the OFDM blocks.

At the receiver the forward transform is performed by the FFT block on the received data for each symbol as

$$R_k = \frac{1}{\sqrt{N}} \sum_{m=0}^{N-1} r_m \exp\left(\frac{-j2\pi km}{N} \right) \qquad for\ 0 \le k \le N-1 \tag{3.5}$$

where, $r = \left[r_0\ r_1\ r_2 \cdots r_{N-1} \right]^T$ is the time-domain vector representing the sampled time-domain signal at the input to the FFT at receiver, and $R = \left[R_0\ R_1\ R_2 \cdots R_{N-1} \right]^T$ is the discrete frequency-domain vector at the output of FFT. Only N samples are required per OFDM symbol (excluding cyclic prefix).

In the absence of noise and distortion in the channel and/or the front ends of the transmitter and receiver, then the transform pairs of FFT and IFFT are $R = X$ [4].

Now if additive-white-Gaussian-noise (AWGN) is added to the signal, but considering no distortion then the signal obtained is

$$r_m = x_m + w_m \tag{3.6}$$

where, w_m is the AWGN sample, substituting Eq. (3.6) in Eq. (3.5), and rearrangment gives

$$R_k = \frac{1}{\sqrt{N}} \sum_{m=0}^{N-1} r_m \exp\left(\frac{-j2\pi km}{N}\right) = X_k + W_k \qquad for\ 0 \le k \le N-1 \tag{3.7}$$

where,

$$W_k = \frac{1}{\sqrt{N}} \sum_{m=0}^{N-1} w_m \exp\left(\frac{-j2\pi km}{N}\right) \qquad for\ 0 \le k \le N-1 \tag{3.8}$$

W_k is the noise in the k^{th} output obtained from the receiver FFT. Since, every value of W_k is the addition of N independent samples of AWGN, w_m [29]-[31]. In most cases, when the distribution of the time-domain noise w_m is not Gaussian, even then due to the application of central limit theorem, the noise W_k in frequency domain will have Gaussian distribution. The result is that the performance of OFDM systems now depend on the average noise power, unlike conventional serial systems where the performance is limited by the peak values of the noise [4], [10].

Let $x(i) = [x_0(i)\, x_1(i)\, x_2(i) \cdots x_{N-1}(i)]^T$ is the output of the IFFT block in the i^{th} symbol period. In OFDM systems, a cyclic-prefix (CP) is added to the beginning of each time-domain OFDM symbol before transmitting it [32]. A number of samples of the symbol from the end are added to the beginning of the symbol. So, now instead of transmitting

$$x(i) = \left[x_0(i)\, x_1(i)\, x_2(i) \cdots x_{N-1}(i)\right]^T \tag{3.9}$$

the sequence $$x_{CP}(i) = \left[x_{N-G}(i) \ldots\ x_{N-1}(i)\, x_0(i) \ldots x_{N-1}(i)\right]^T \tag{3.10}$$

is transmitted; where G denotes the length of the CP. Although some redundancies are introduced and the overall data rate is reduced, it has been observed that the use of CP eliminates both inter-symbol-interference (ISI) and inter-carrier-interference (ICI) from the received signal and also simplifies equalization in OFDM [1], [4], [27], [33]-[34]. Fig. 3.3 shows the time-domain sequence of OFDM symbols.

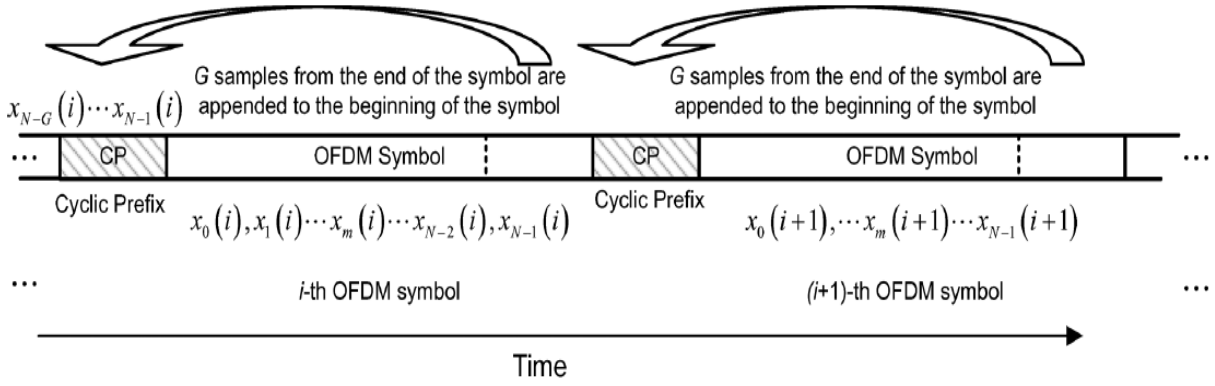

Fig. 3.3. Representation of OFDM symbols with the cyclic prefix in time-domain [4].

The reasons for the usage of cyclic-prefix instead of the guard interval are [4]:

- It maintains the receiver carrier synchronization because some signal is always being transmitted instead of a long silence.
- Cyclic convolution is still applied between the OFDM signal and the channel response to model the transmission system.

OFDM is widely used because of the fact that, when a CP is used, any distortion that is caused by the linear dispersive channel can simply be corrected by a 'single-tap' equalizer [4]. Consider there is perfect up conversion and down conversion where the received signal is the sum of two versions of the transmitted signal with different gains and delay.

$$r(t) = g_1 x(t+\tau_1) + g_2 x(t+\tau_2) \tag{3.11}$$

For every OFDM symbol, the FFT has N input samples from the signal within the indicated time period in Fig. 3.4. It is shown that if the beginning of receiver time window is aligned to the beginning of the OFDM symbol of the first received signal, and if the delay spread (τ_2-τ_1) is less than the length of the cyclic prefix, there is minimal to zero ISI. The signal received in the i^{th} time window depends only on the i^{th} transmitted symbol.

Inter-symbol-interference can also be eliminated by appending a guard interval before each OFDM symbol in which no signal is transmitted, but it results in inter-carrier-interference (ICI). Each value of R_k depends on input values X and not on X_k. Therefore as long as the delay spread in the channel is less than the CP, and the FFT window is aligned

with the beginning of the main symbol period of the first received signal, then no ISI or ICI occurs [35].

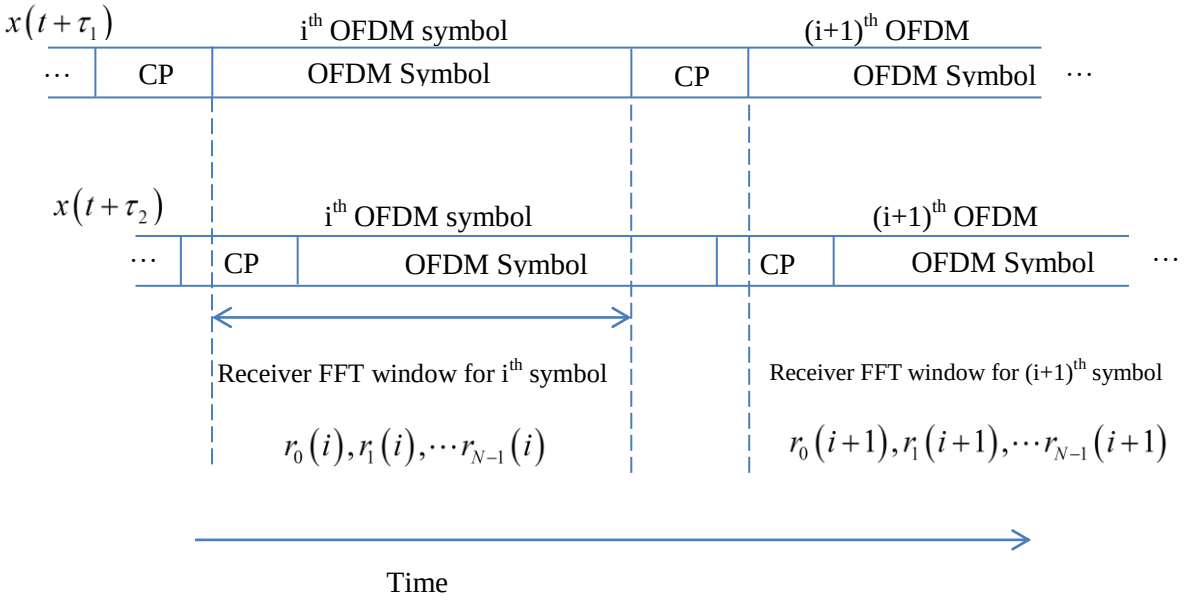

Fig. 3.4. OFDM symbols in a multipath channel: two components of the received signal with different delays [4].

Now, considering the effect of a dispersive channel on a single subcarrier analytically. To simplify, ignore the effects of noise. Considering the range till the Nyquist term i.e., $k = N/2$ for simplified discussion

Let the continuous baseband signal at the transmitter associated with the k^{th} subcarrier of a given OFDM symbol (including the CP) be

$$x(k,t) = \frac{1}{\sqrt{N}} \sum_{k=0}^{N-1} X_k \exp\left(\frac{j2\pi kt}{T}\right) \qquad for\ 0 \le k \le \frac{N}{2} - 1 \tag{3.12}$$

Then, the received continuous time-domain signal for the two path channel described in Eq. (3.11) is

$$r(k,t) = \frac{1}{\sqrt{N}} g_1 X_k \exp\left(\frac{j2\pi k(t-\tau_1)}{T}\right) + \frac{1}{\sqrt{N}} g_2 X_k \exp\left(\frac{j2\pi k(t-\tau_2)}{T}\right) \qquad for\ 0 \le k \le \frac{N}{2} - 1 \tag{3.13}$$

Ideally the receiver is synchronized, so that the FFT window is aligned with the beginning of the symbol period for the first arriving version of the transmitted signal. So for this case, the receiver FFT window is offset by τ_1. So

$$r(k,t) = \frac{1}{\sqrt{N}} g_1 X_k \exp\left(\frac{j2\pi kt}{T}\right) + \frac{1}{\sqrt{N}} g_2 X_k \exp\left(\frac{j2\pi k\left(t-\left(\tau_2-\tau_1\right)\right)}{T}\right) \tag{3.14}$$

$$r(k,t) = \frac{1}{\sqrt{N}} X_k \exp\left(\frac{j2\pi kt}{T}\right) \times \left(g_1 + g_2 \exp\left(\frac{-j2\pi k\left(\tau_2-\tau_1\right)}{T}\right)\right) \tag{3.15}$$

So after demodulation by the FFT and including the effect of noise, it can be shown that

$$R_k = X_k\left(g_1 + g_2 \exp\left(\frac{-j2\pi k\left(\tau_2-\tau_1\right)}{T}\right)\right) + W_k \tag{3.16}$$

$$R_k = X_k H_k + W_k \tag{3.17}$$

where,

$$H_k = g_1 + g_2 \exp\left(\frac{-j2\pi k\left(\tau_2-\tau_1\right)}{T}\right) \tag{3.18}$$

The transmitted data can be recovered from the received signal by multiplying R_k with $1/H_k$. That is each subcarrier can be recovered using one complex multiplication. This is the role of the single-tap equalizer.

$$\hat{X}_k = \frac{R_k}{H_k} = X_k + \frac{W_k}{H_k} \tag{3.19}$$

3.3.1 Orthogonality Property of OFDM

The subcarriers are chosen to be orthogonal by carefully selecting the carrier spacing such that it is equal to the inverse of the symbol period. With the orthogonality between the subcarriers, there will be a null at the centre frequency of each subcarrier in the spectrum. Thus, the interference between the subcarriers is removed and allowing overlapping between adjacent subcarriers. Mathematically, the orthogonality can be stated as

$$\int_0^T \psi_p(t)\psi_p^*(t)\,dt = \begin{cases} k & if\ p = q \\ 0 & if\ p \neq q \end{cases} \tag{3.20}$$

where, ψ_p and ψ_q are two signals, and T is the symbol time-period over which orthogonality is to be checked. When the integral calculates to zero, the signals are said to be orthogonal. If the subcarriers are orthogonal, the peaks of one subcarrier will occur on the null of other subcarriers. This enables in extraction of the data from the overlapping subcarriers. The carrier spacing must be chosen carefully for attaining the orthogonality between subcarriers. The subcarriers in the OFDM symbol are chosen with carrier spacing as $\Delta f = \frac{1}{NT_s} = \frac{1}{T}$, where T is the duration of the symbol [1]. The frequency spectrum of the OFDM symbol is shown in Fig. 3.5.

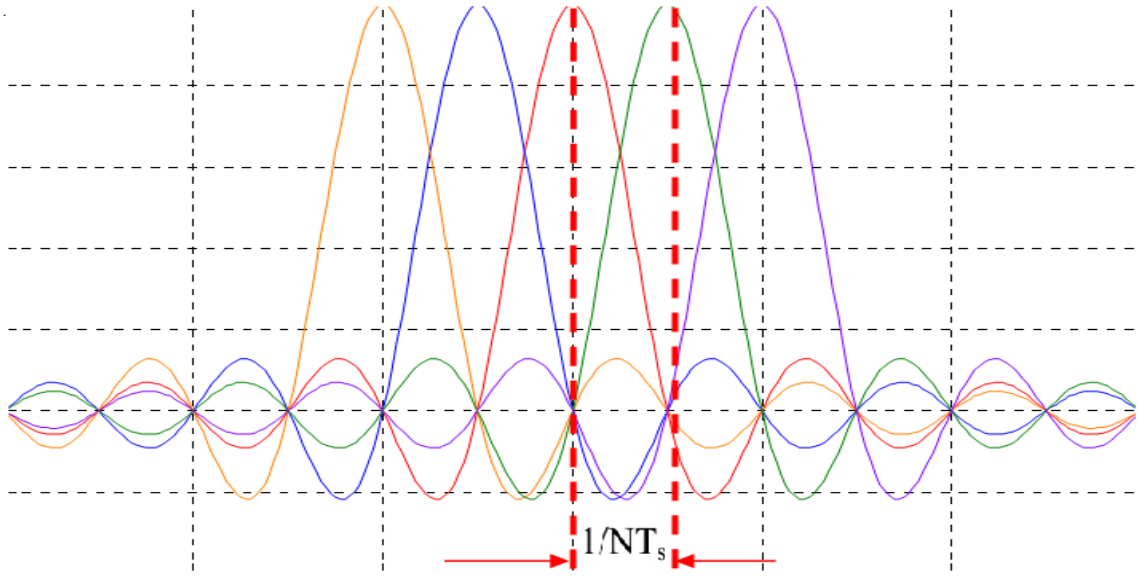

Fig. 3.5. Orthogonal subcarriers in OFDM symbol [1].

3.4 Implementation of OFDM

The performance of the OFDM system is simulated and analysed under the influence of AWGN, also called thermal noise, working on different fading conditions, modulation schemes and number of subcarriers in each OFDM symbol. The plot for BER vs. SNR is demonstrated to study the performance obtained.

3.4.1 Simulation Model for OFDM System

The OFDM system is simulated using MATLAB software. The analysis of the system is done by studying the plot obtained between BER and SNR (dB) under different modulation techniques, fading conditions and number of subcarriers. One of the most important advantages obtained when using OFDM is its ability to convert the frequency-selective fading channel into flat fading channel. This is accomplished by transmitting data in parallel across N subcarriers as opposed to single carrier methods that use the entire bandwidth available [36]-[37].

The block diagram for the OFDM system used under simulation is shown in Fig. 3.6. This section discusses each of the block shown in Fig. 3.6.

- **Data Generator**

  The data that is to be transmitted on different subcarriers is modulated to any of the modulation schemes like quadrature-amplitude-modulation (QAM) or quadrature-phase-shift-keying (QPSK). As the degree of the QAM scheme increases, the data bits come closer to each other on the constellation diagram when keeping the total power constant. QPSK keeps the amplitude of all the data bits at equal levels but for 16-QAM and 64-QAM, the amplitude for the data bits for different coded data is different.

- **Serial-to-Parallel Convertor**

  The data received after modulation is in series and has to be converted to parallel to be fed into the IDFT block. So after modulation, the data blocks are fed into the serial-to-parallel convertor to obtain parallel data of block size N, equal to the size of IDFT/DFT block size or the number of subcarriers used in OFDM symbol.

- **Inverse-Discrete-Fourier-Transform (IDFT)**

  IDFT/DFT is obtained using the IFFT/FFT algorithms for easier, low complexity and faster computations. IDFT is used at the transmitter to convert the frequency-domain data-stream into time-domain data-stream.

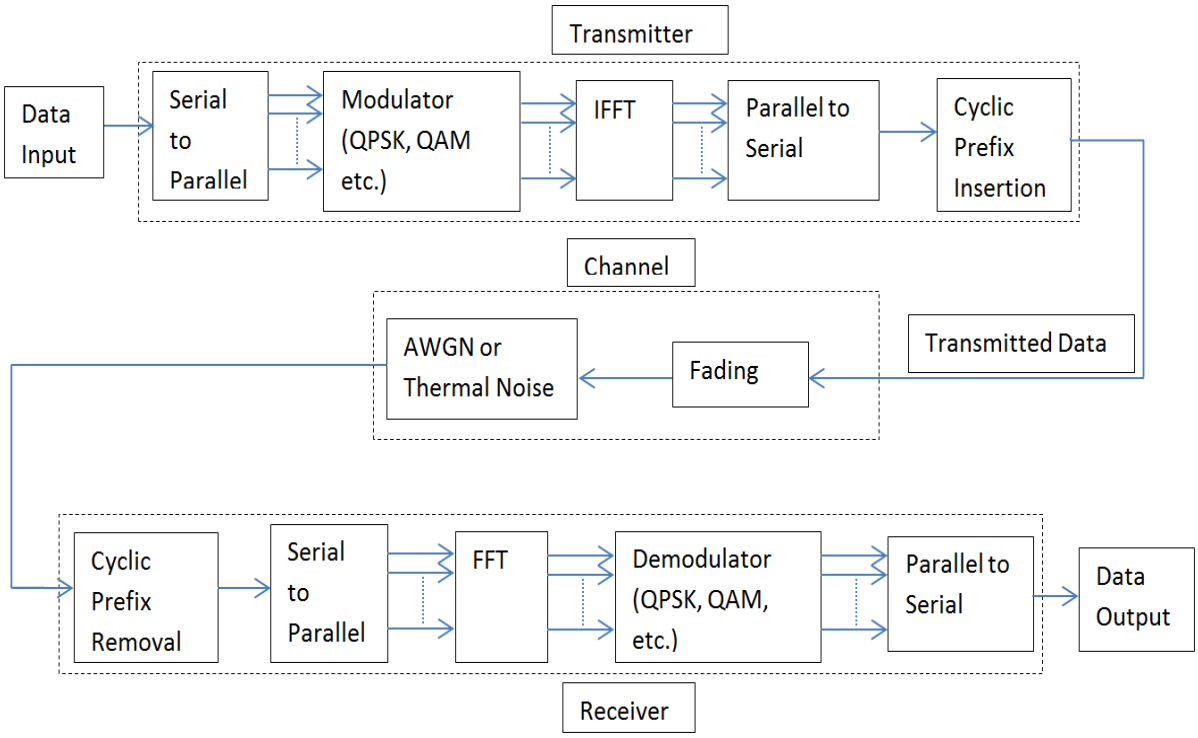

Fig 3.6. Block diagram depicting the OFDM system under simulation [36].

- **Cyclic Prefix**

  Cyclic prefix is added to the time-domain data stream obtained from the IDFT block. It eliminated the severe effects of inter-symbol-interference (ISI). The length of the cyclic prefix to be used in the OFDM system is decided based on the delay spread in the channel. The length of CP is increased if the channel offers greater delay spread and vice versa.

- **Channel**

  The frequency-selective channel when acts upon the OFDM transmitted data-stream, it is experienced as flat fading channel because the parallel subcarriers experience fading independently. The AWGN or thermal noise is also added in the channel.

- **Receiver**

  At the receiver, all the tasks performed at the transmitter are performed in reverse to obtain the original data-stream. First cyclic prefix is removed, followed by conversion

to frequency-domain by the DFT block using FFT algorithms. This data-stream is then demodulated back to original symbols.

3.4.2 Simulation Results and Discussion

The results obtained are for the configurations explained as follows:

- **Case 1:** OFDM system performance under different modulation schemes

In this simulation, the effect of different modulation schemes on the performance of OFDM system is observed. The system is simulated using QPSK, 16-QAM and 64 QAM modulation schemes with 256 subcarriers in each OFDM symbol [38], [39]. The average value for a channel-tap coefficient is kept fixed at 0.75. The bit-error-rate (BER) versus signal-to-noise-ratio (SNR) is plotted using the parameters summarized as follows in Table 3.1.

As shown in Fig. 3.7, the performance of the OFDM system gets degraded with increase in the order of modulation scheme. As the constellation points increases at the constant power level, the Euclidean distance between neighbouring points decreases. It leads to increase in BER But with increase in the order of modulation, the data rate increases. So, there exists a trade-off between the data rate required and the acceptable level of error tolerance.

Table 3.1. OFDM parameters for simulation under different modulation schemes.

Parameter	**Value**
Modulation used	QPSK, 16-QAM, 64-QPSK
Number of subcarriers	256
Average value for a single channel-tap coefficient $\left(H_{avg}\right)$	0.75
SNR	0 to 20

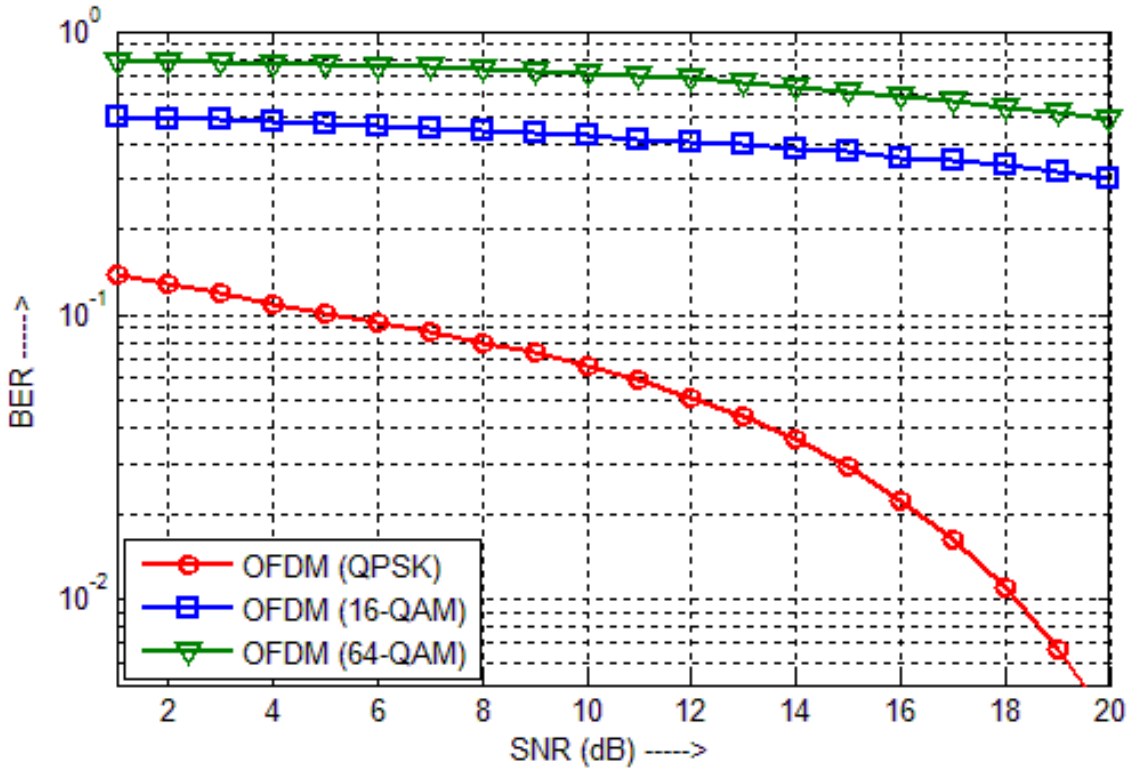

Fig. 3.7. BER vs. SNR (dB) with different modulation schemes.

- **Case 2:** OFDM system performance under different fading conditions

Further, the OFDM system is subjected to different fading conditions by varying the channel tap-coefficient in frequency-domain $H_{avg} \Rightarrow \{0.5, 0.75, 1\}$; where $H_{avg} = 1$ denotes the condition with no fading. The modulation used is 16 QAM with 256 subcarriers in each OFDM symbol. The bit-error-rate versus signal-to-noise-ratio is plotted with the parameters summarized in Table 3.2.

As shown in Fig. 3.8, the performance of the OFDM system degrades with decreasing value of the channel tap-coefficient. When channel parameter H is equal to 0.5 i.e., under fast fading conditions, the performance is worst. The subcarriers in such conditions are received with high error rates and may be rendered useless.

Table 3.2. OFDM parameters for simulation under different fading conditions.

Parameter	**Value**
Modulation used	16-QAM
Number of subcarriers	256
Average value for a single channel-tap coefficient $\left(H_{avg}\right)$	0.5, 0.75, 1
SNR	0 to 30

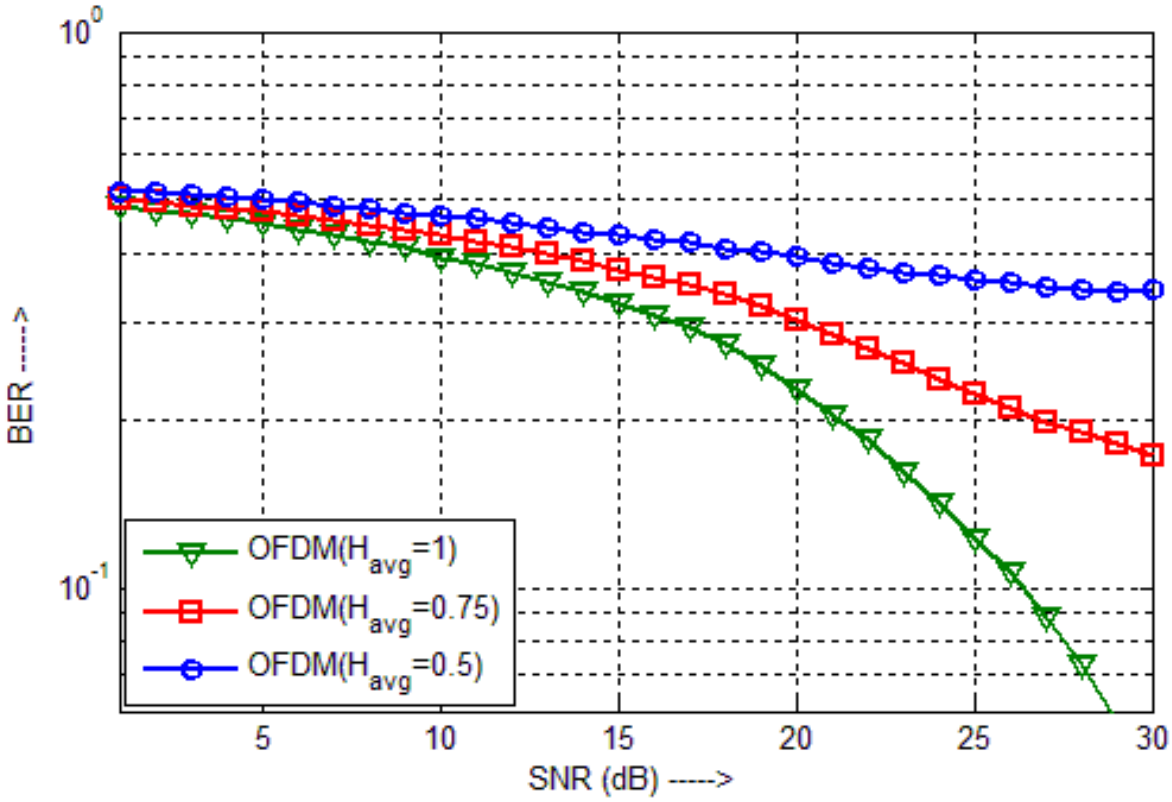

Fig. 3.8. BER vs. SNR (dB) under different fading conditions.

- **Case 3:** OFDM system performance under different number of subcarriers

In this simulation, the OFDM system is studied while varying the number of subcarriers. The modulation scheme used is 16-QAM with channel tap-coefficient in frequency-domain kept constant at 0.75. The bit-error-rate versus signal-to-noise-ratio is plotted with the parameters summarized in Table 3.3.

As shown in Fig. 3.9, the performance of the OFDM system degrades with increasing value of the number of subcarriers. As the number of subcarriers increases, the noise is spread across all the subcarriers due to the spreading effect of IDFT/DFT and the demodulation introduces errors in all the bits in a symbol under the noisy conditions.

Table 3.3. OFDM parameters for simulation under different number of subcarriers.

Parameter	**Value**
Modulation used	16-QAM
Number of subcarriers	64, 256, 1024
Average value for a single channel-tap coefficient $\left(H_{avg}\right)$	0.75
SNR	0 to 40

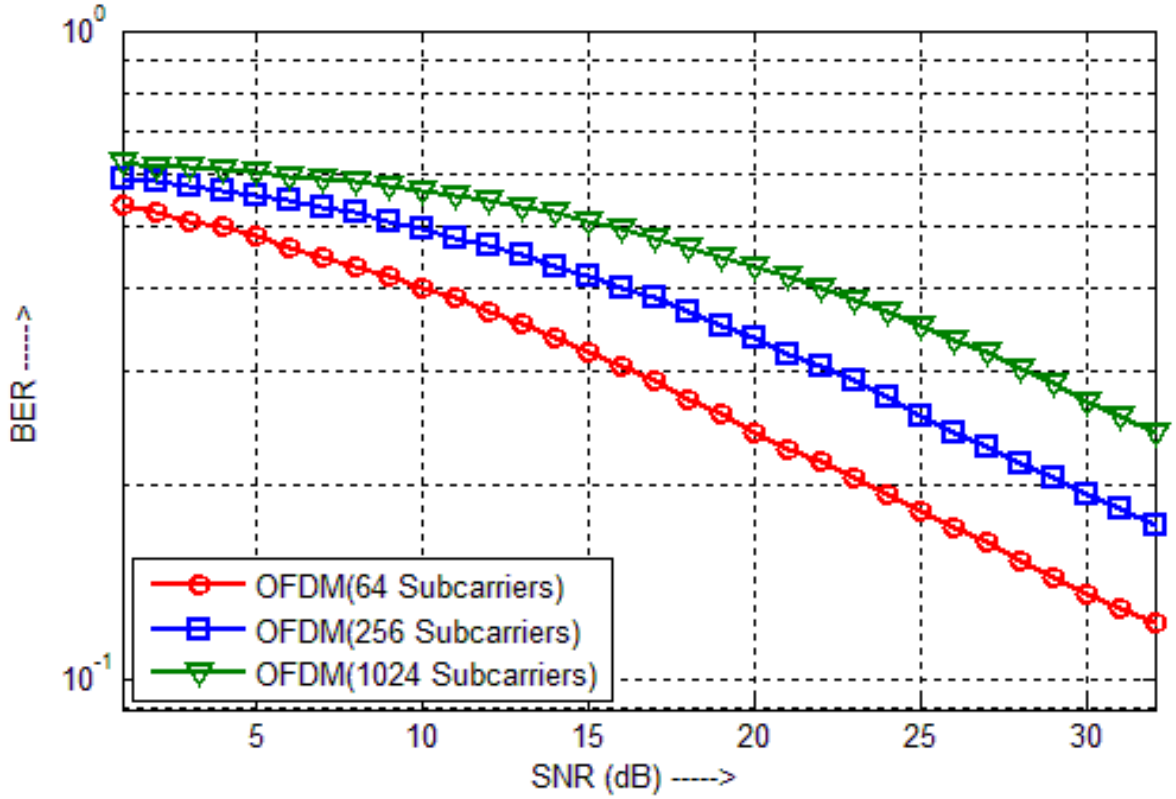

Fig 3.9. BER vs. SNR (dB) with different number of subcarriers.

3.5 Advantages of OFDM

- OFDM can be efficiently implemented using IFFT/FFT algorithms. OFDM inherits the spreading effect due to IDFT/DFT with lower computational complexity.
- It is more immune to impulsive noise with low amplitudes and co-channel interference [4], [12].
- Inter-symbol-interference and inter-carrier-interference are effectively eliminated in OFDM [4].
- It is spectral efficient with the overlapping of subcarriers, saving bandwidth while transmitting data at high data rates [40]-[41].
- It provides immunity to frequency-selective fading as it breaks the channel into narrow band carriers, thus converting frequency-selective fading to flat fading [29], [41].

3.6 Limitations of OFDM

The limitations of OFDM system are synchronization and nonlinearity.

- The process of timing synchronisation includes the detection and adjustment of the receiver to the beginning of the symbol. If some mismatch occurs within the cyclic prefix, it introduces only linear phase error that can be corrected with ease at the output obtained from the DFT by the estimators. On the other hand, mismatch in the synchronisation results in interference [1]-[2], [4].
- The mismatch in the synchronisation at the RF oscillator between the transmitter and receiver results in phase noise in subcarriers [29].
- With the mismatch between the RF oscillators and Doppler shifts due to channel impairments results in frequency offsets [29].
- The OFDM system suffers from peak-to-average-power-ratio (PAPR) due to high instantaneous peaks occurring in the symbol relative to the average signal power [1], [4], [29].

Chapter 4

IMPULSIVE NOISE MITIGATION TECHNIQUES UNDER FADING ENVIRONMENT

This chapter discusses the fading that is introduced in the channel and different types of multipath fading. It also includes brief summary about the impulsive noise, its mathematical modelling. Further, the chapter gives details about the modelling of impulsive noise in this work and the brief discussion about the two impulsive noise suppression schemes that are analysed, compared and optimized.

4.1 Fading

Fading is a very severe problem in wireless communication. It causes variation in the strength of signal by affecting multipath delay, phase or amplitude over a short duration of time. Two or more versions of the same transmitted signal arriving at the receiver with some time gap interfere with each other. This induces fading.

Fading is produced by many factors like reflection, diffraction, scattering, refraction. Reflection takes place when the electromagnetic wave travelling in the channel impinges on any object whose dimensions are very large as compared to the wavelength of the wave. This is observed when the radio waves get reflected from the earth. This causes a change in the polarization of the reflected waves. This change in the polarisation of the signal affects the antennas at the receiver due to their inability to detect the received signal with changed polarisation.

When the channel between the transmitter and receiver has sharp peaks, the signal diffracts when striking on these irregularities. Fading occurs due to the absorption of signal's RF energy when travelling through the ionosphere. For longer periods, the fading is mainly of absorption type. The reflection of the signal from the building and other structures in the path of the signal causes multipath and delays [42].

4.1.1 Path Loss

The power of the signal received depends on the distance between the transmitter and receiver. As the distance between the two increases, the energy of the received signal decreases. Path loss may be defined as this difference between the power of the transmitted

signal and the received signal [42]-[43]. This attenuation of signal is a positive quantity, which is measured in dB. In the case of free space, when direct line-of-sight (LOS) is assumed between the transmitter and receiver, there are no secondary waves generated from the reflections from medium objects; and the power of received signal is found to be inversely proportional to the square of the distance between then transmitter and receiver and also to the square of the carrier frequency [42]. The relationship can be expressed as

$$P_R \propto \frac{GP_T}{f^2 d^a} \tag{4.1}$$

where, P_R and P_T are the powers associated with the received signal and transmitted signals, f is the carrier frequency, d denotes the distance between the transmitter and receiver, a is the path loss component, G is the power gain. The path loss can be modelled as

$$PL(dB) = 10\log\frac{P_T}{P_R} = -10\log\left[\frac{G_T G_R \lambda^2}{(4\pi)^2 d^2}\right] \tag{4.2}$$

where, PL is the path loss expressed in dB.

4.1.2 Shadowing Effect

Shadowing effect expresses the fluctuations in the power of the received signal when it encounters objects in the channel obstructing its path. The variations and fluctuations in the power of received signal are dependent on the surroundings and the prevailing conditions of the transmitter and receiver. The performance of the wireless communication system declines if the variations encountered by the transmitted signal are large.

The path loss for the system is measured in dB. Though the path loss is random, but on log scale it has log normal distribution. When evaluating the path loss, the equation does not take into consideration the environmental factors and conditions because they have dependence on the location and distance of the transmitter and receiver. For shadowing effects, the log normal describes the shadowing that occurs for constant distance between the transmitter and receiver but with different location conditions. Table 4.1 accounts for the attenuation occurring due to shadowing effects in a dense urban area, sub-urban area and rural area.

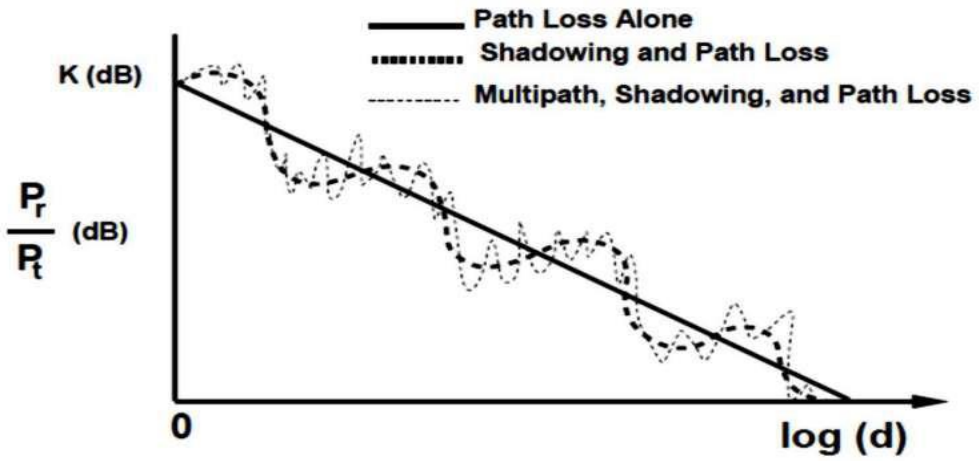

Fig. 4.1. Power ratio of received to transmitted signal vs. the distance between the transmitter and receiver [43].

Table 4.1. Attenuations due to shadowing in radio channel.

Location	**Attenuation due to shadowing**
Urban area	20 dB attenuation variation from street to street
Sub-urban area	10 dB less attenuation from urban areas
Open rural area	20 less attenuation from urban areas
Terrain irregularities	3-12 dB attenuation variations

4.2 Multipath Fading

The path between the transmitter and receiver has reflecting objects and scatters that constantly deflect and reflect the signal dissipating its energy in terms of amplitude, phase and time. This results in multiple versions of the transmitting signal travelling through the channel and interfering with each other when arriving at the receiver. This is taken into account by considering multipath fading in a radio communication system. In terrestrial communication system, the transmitted signal reaches the receiver along with its multiple versions along multiple paths. This is mainly caused by reflections from the objects

obstructing the path between the transmitter and receiver, which includes hills, buildings, vehicles, surfaces, moving objects and ground etc. A case of signal following multipath is shown in Fig. 4.2.

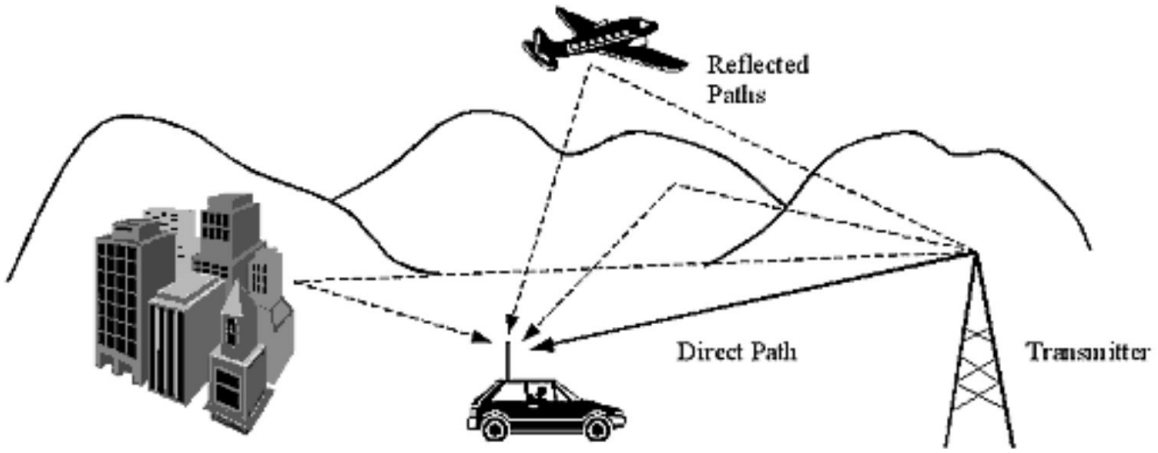

Fig.4.2. Multipath fading channel [43].

The resultant signal consisting of multiple versions of the same transmitted signal travelling along multiple independent paths reaches the receiver, they have different path lengths. This results in interference in the signal, which may be constructive or destructive depending on the relative phases between each of the versions.

The path between transmitter and receiver contains moving objects that provide surface for reflection for the signal. This results in the change of relative path lengths for signal. This varying path lengths result in phase shifts in different versions of the signal arriving at the receiver. The constructive or destructive interference in these signals result in variation in the signal strength. This is a major factor in fading of the signal on radio communication channels. Problems like ISI and phase distortion are also encountered. These problems needs to be addressed and proper mitigating methods are to be applied. There are different types of fading that are encountered. These are now discussed.

4.2.1 Types of Multipath Fading

The propagation models for signal take into account the average signal strength at the receiver for a specified distance from the transmitter and also the variations in the signal strength observed in close proximity to a specified location. Multipath fading can be classified into different types depending on the conditions. This is shown in Fig. 4.3.

The main classification of multipath fading is

- Large Scale Fading
- Small Scale Fading

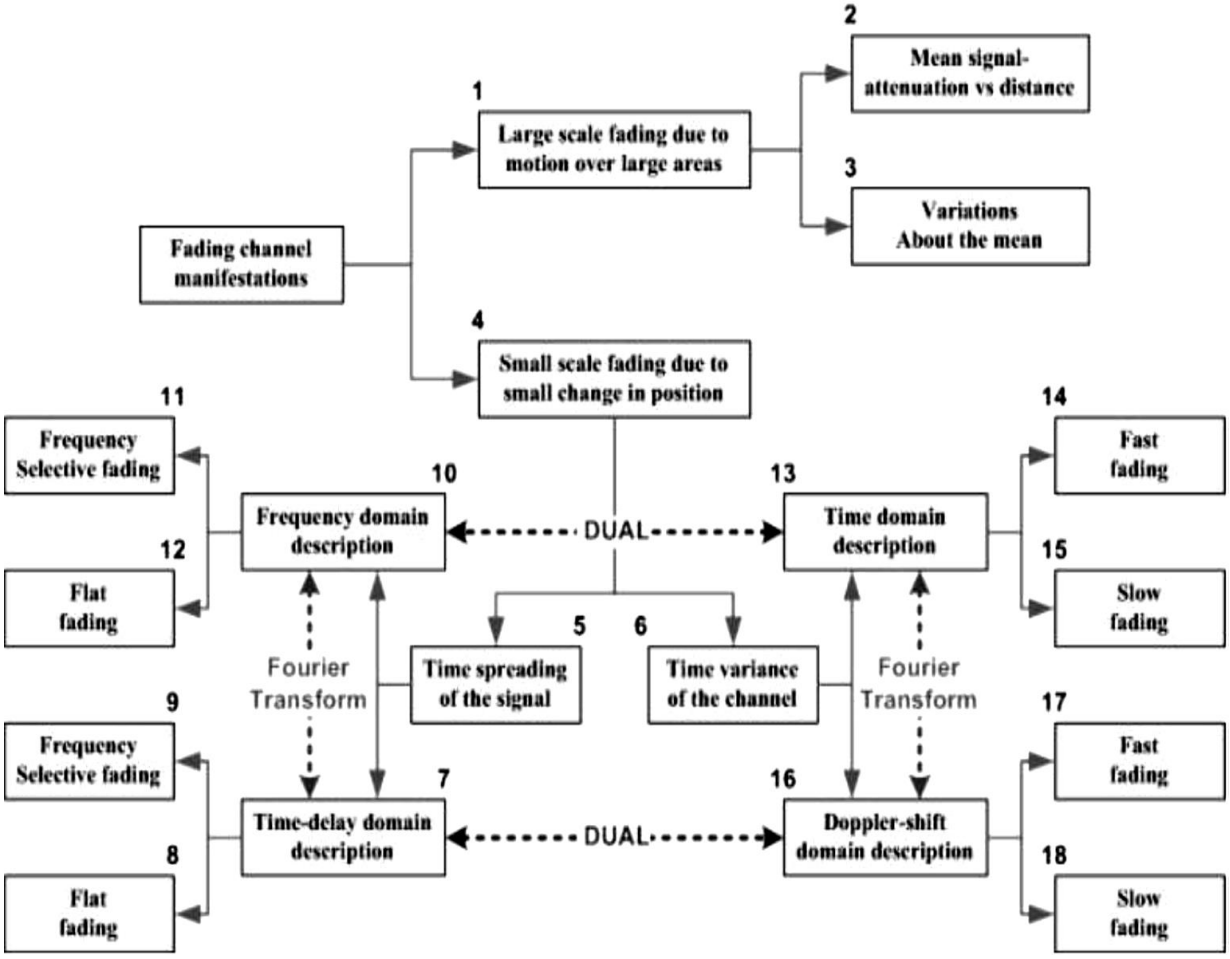

Fig.4.3. Different types of multipath fading [43].

4.2.1.1 Large Scale Fading

Mean signal strength between transmitter and receiver with arbitrary distance is a very important parameter for estimating the coverage area for the transmitter. Propagation models are hence important for studying the effects of the channel on transmitted signal. For large scale propagation models, the signal strength over large distances between the transmitter and receiver (of the order of hundreds or thousands of kilometres) is characterised. As the mobile receiver moves away from the transmitter, the signal strength of the received signals decreases with the increase in distance. This is due to the absorption of the RF energy of the signal in the ionosphere. Reflection, scattering and diffraction are the main reasons for the absorption of the signal. The large scale fading can be modelled by different models like Longley-Rice model, Hata model, Okumura model, Durkin's model etc.

4.2.1.2 Small Scale Fading

Propagation model for small scale fading characterize the signal strength for small distances between the transmitter and receiver. The instantaneous fluctuations in the signal over short distances are very rapid when the mobile receiver is moving away from the transmitter. This gives rise to small scale fading. For small scale fading, the fluctuation in the signal strength can be in the order of three or four in the magnitude (30dB to 40dB), when the movement is only a fraction of the wavelength. The relation between large scale fading and small scale fading is shown in Fig. 4.4. Fig 4.4 (a) shows the variation with respect to distance in both large scale fading m(t) and small scale fading r(t). Fig. 4.4 (b) shows only the small distance fading $r_o(t)$. Small scale fading is further classified on the bases of the impulse response of the fading channel into multipath delay spread and Doppler spread. Small scale fading can also be classified as fast fading and slow fading, and flat fading and frequency-selective fading.

4.3 Types of Small-Scale Fading

The transmitted signal and the channel characteristics play an important role in type of fading that the signal will experience while propagating through the radio channel. Signal parameters like bandwidth and signal power also play an important role. Channel parameters like the delay and Doppler shifts also needs to be known for finding the type of fading experienced by the signal [43].

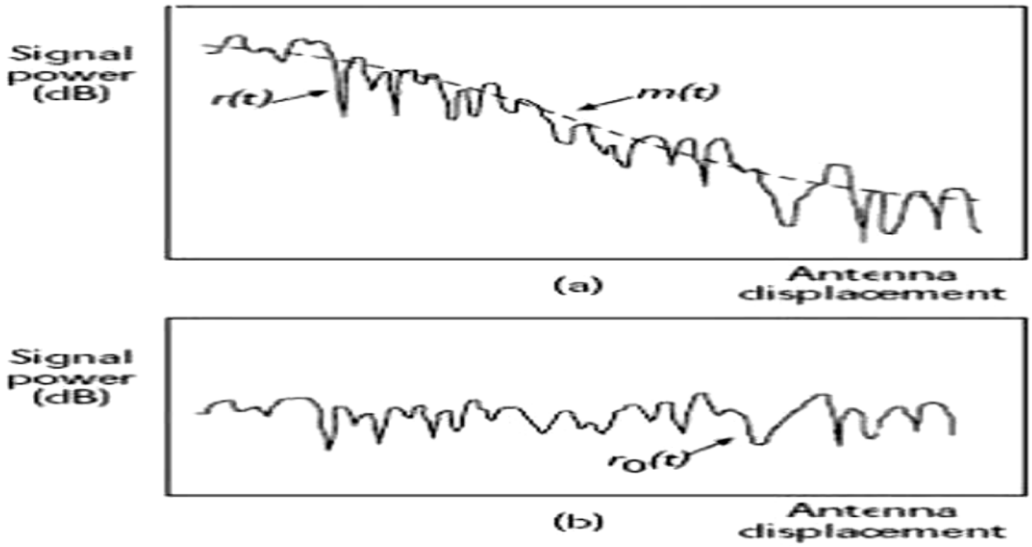

Fig. 4.4. Small scale and large scale fading [43].

Now, the different types of small scale fading are discussed

- Flat Fading
- Frequency-selective fading
- Fast fading
- Slow fading

4.3.1 Flat Fading

The signal experiences flat fading when the channel has a constant gain and has a linear phase response over a bandwidth which must be more than the bandwidth of the signal that is being transmitted. The transmitted signal's characteristics are preserved, when it reaches the receiver. The amplitude experiences some variations due to fluctuations in the channel gain caused by the multipath. Mathematically, flat fading is experienced, when the following conditions are present for the channel.

$$B_s \ll B_c \tag{4.3}$$

and

$$T_s \gg \sigma_\tau \tag{4.4}$$

where, B_s is the bandwidth for the transmitted signal, B_c is the coherence bandwidth for the channel, T_s is the reciprocal of the bandwidth for the signal, σ_τ is the RMS delay spread [42]-[43].

4.3.2 Frequency-Selective Fading

The signal experiences frequency-selective fading when the channel has a constant gain and has a linear phase response over a bandwidth which must be less than the bandwidth of the signal that is being transmitted. The transmitted signal's characteristics are not preserved when it reaches the receiver. The amplitude experiences some variations due to fluctuations in the channel gain caused by the multipath. Mathematically, frequency-selective fading is experienced when the following conditions are present for the channel.

$$B_s \gg B_c \tag{4.5}$$

and

$$T_s \ll \sigma_\tau \tag{4.6}$$

where, B_s is the bandwidth for the transmitted signal, B_c is the coherence bandwidth for the channel, T_s is the reciprocal of the bandwidth for the signal, σ_τ is the RMS delay spread.

For modelling frequency-selective fading, each multipath must be modelled separately keeping the phase linear for the channel. This makes the modelling for frequency-selective fading much more difficult than the modelling for flat fading channel [27], [42]-[43].

4.3.3 Fast Fading

Fast fading and slow fading are dependent on the rate at which the transmitted signal changes as compared to the rate at which the channel changes. When the channel impulse response varies rapidly in the symbol duration, the signal experiences fast fading. Fast fading causes the frequency dispersion in the signal due to Doppler spreading. This leads to large distortions in the transmitted signal. The distortion in the signal increases with the increase in the Doppler's spread for the channel. Mathematically, the conditions when the signal experiences fast fading can be expressed as

$$T_s \gg T_c \tag{4.7}$$

and

$$B_s \ll B_D \tag{4.8}$$

where, B_s is the bandwidth for the transmitted signal, B_D is the Doppler's spread for the channel, T_s is the reciprocal of the bandwidth for the signal, T_c is the reciprocal of the coherence bandwidth [42]-[43].

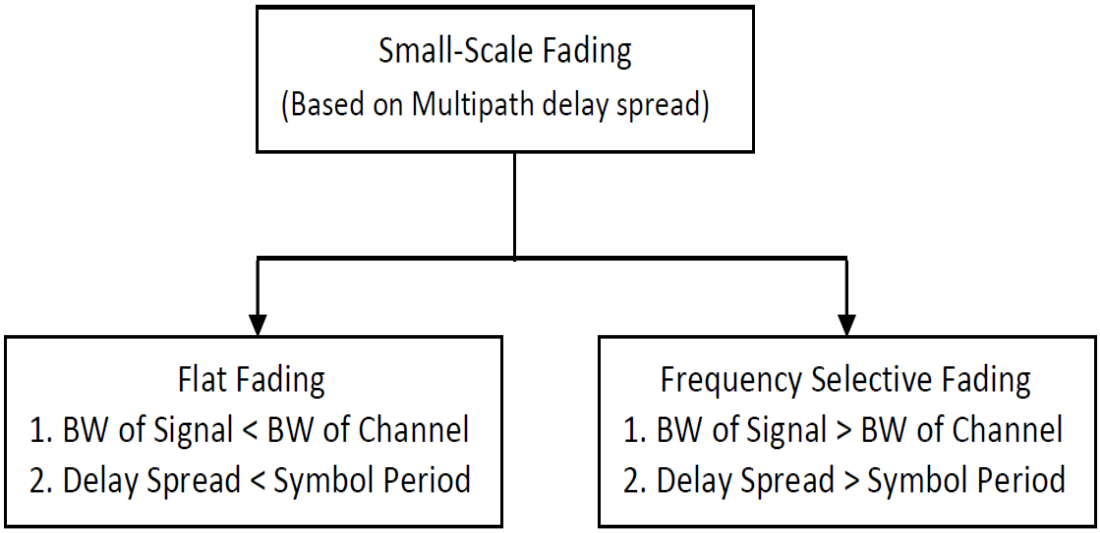

Fig. 4.5 (a). Classification of small scale fading based on multipath delay [43].

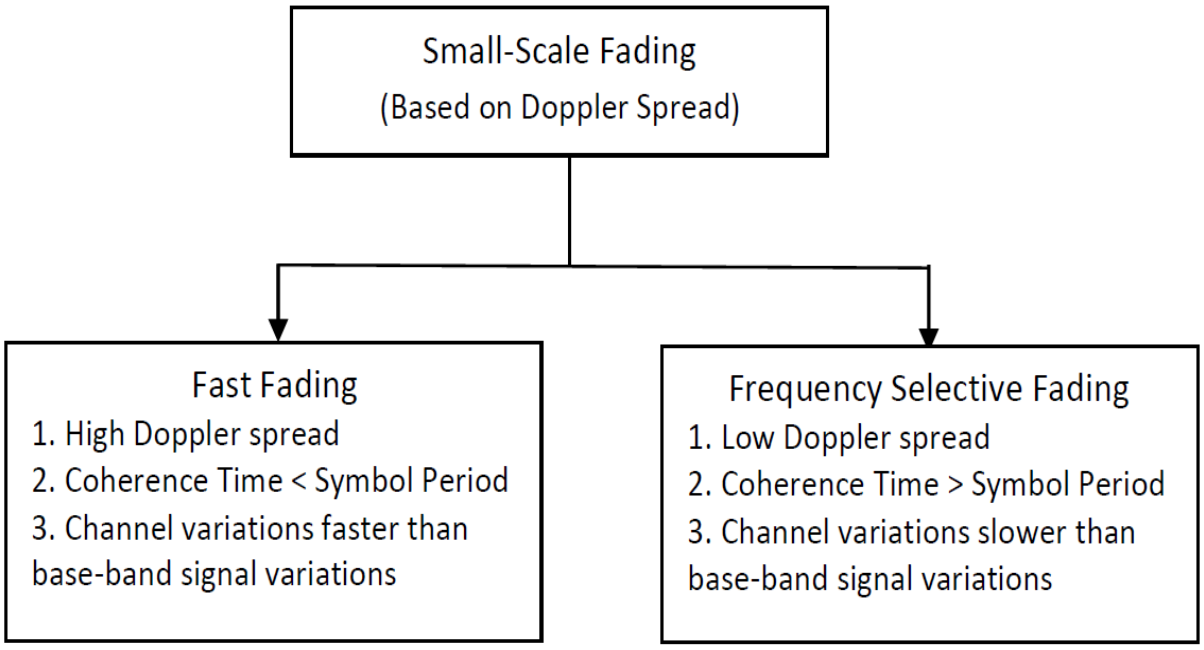

Fig.4.5 (b). Classification of small-scale fading based on Doppler's spread [43].

4.3.4 Slow Fading

When the channel impulse response varies rather slowly than the rate of the transmitted signal, it experiences slow fading. The bandwidth of the transmitted signal is greater than the Doppler's spread of the channel. Mathematically, the conditions when the signal experiences slow fading can be expressed as

$$T_s \ll T_c \tag{4.9}$$

and

$$B_s \gg B_D \tag{4.10}$$

where, B_s is the bandwidth for the transmitted signal, B_D is the Doppler's spread for the channel, T_s is the reciprocal of the bandwidth for the signal, T_c is the reciprocal of the coherence bandwidth [42]-[43].

The types of small scale fading can be summarized by Fig 4.5.

4.4 Impulsive Noise Model

Impulsive noise is a train of one or more repetitive pulses with varying duration, occurrence and intensity. Impulsive noise consists mainly of short duration on/off pulses produced by varied sources like clicks from computer, sharp sounds, vehicular ignition systems, mechanical sounds, adverse channel conditions, switching sounds etc. [44].

For improving the performance of system, it is preferred to remove impulsive noise from the received signal. Different characteristics of the signal and noise are used at the receiver to detect and remove the effects of impulsive noise in either time-domain or frequency-domain. The statistics of the noise is also used to improve the detection of noise and make the system robust against it [45].

4.4.1 Mathematical Model for Impulsive Noise

A unit area pulse p(t) shown in Fig. 4.6 (a) has a width of Δ tending to zero can be considered as an impulse noise pulse. The impulsive pulse shown in Fig. 4.6 (b) with infinitesimal width can be defined mathematically as

$$\delta(t) = \lim_{\Delta \to 0} p(t) = \begin{cases} 1/\Delta & |t| \le \Delta/2 \\ 0 & |t| > \Delta/2 \end{cases} \tag{4.11}$$

The integral of this impulsive pulse is equal to 1 evaluated as

$$\int_{-\infty}^{\infty} \delta(t)dt = \Delta \times \frac{1}{\Delta} = 1 \tag{4.12}$$

The frequency-domain transformation of the impulsive pulse is represented as

$$\Delta(f) = \int_{-\infty}^{\infty} \delta(t) e^{-j2\pi ft} dt = e^0 = 1 \tag{4.13}$$

The impulsive noise in frequency-domain contains all the frequencies in equal amounts. This makes it a spectrally rich signal. This has been shown in Fig. 4.6.

In the digital domain, impulsive noise is signal of unit amplitude in the sample. It can be expressed as

$$\delta(n) = \begin{cases} 1 & n = 0 \\ 0 & n \neq 0 \end{cases} \tag{4.14}$$

where, n is a discrete variable for discrete-time index.

In practical communication systems, the impulsive noise consists of more than one pulses. For 5 millisecond duration, impulsive noise has 50 pulses at a sampling rate of 50 KHz. The impulsive noise can have originated at any point in the channel randomly. It then propagates to the receiver affected the signal in the channel. The communication channel can be linear/nonlinear or stationary/time-varying.

Impulsive can be classified into two broad categories: periodic impulsive noise and aperiodic impulsive noise. Periodic impulsive noise is characterized by impulse pulses occurring at periodic intervals in time-domain and has long duration. On the other hand, the aperiodic impulse noise has pulses occurring at random instances of time, with shorter durations and higher power. The detection of impulsive noise in frequency-domain is much more difficult as compared to detection in time-domain. Practically, the effects of impulsive noise are reduced over a sample period as opposed to locating and removing individual impulsive noise pulse. The impulsive noise representation in time-domain and frequency-domain is shown in Fig. 4.7.

4.4.2 Gated Gaussian Model for Impulsive Noise

The model of impulsive noise that is commonly and extensively used in transmission models for characterization is the gated Gaussian noise model that breaks down the impulsive noise into two component Gaussian noise.

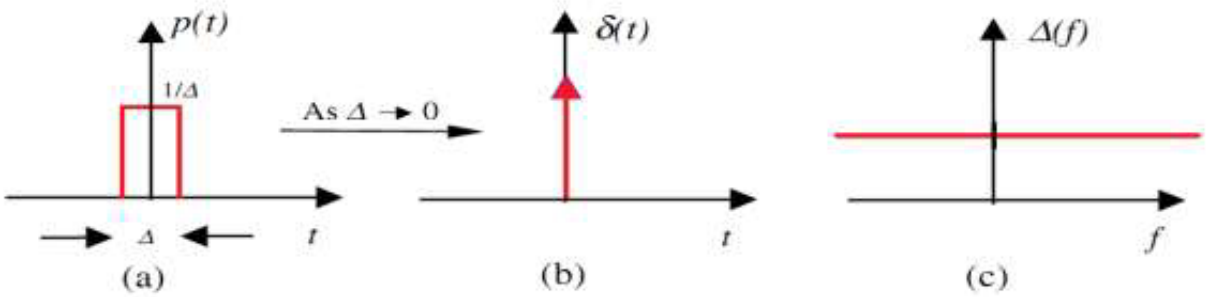

Fig. 4.6 (a). Unit area pulse (b) Impulsive noise pulse with width tending to zero (c) Spectrum of impulsive pulse.

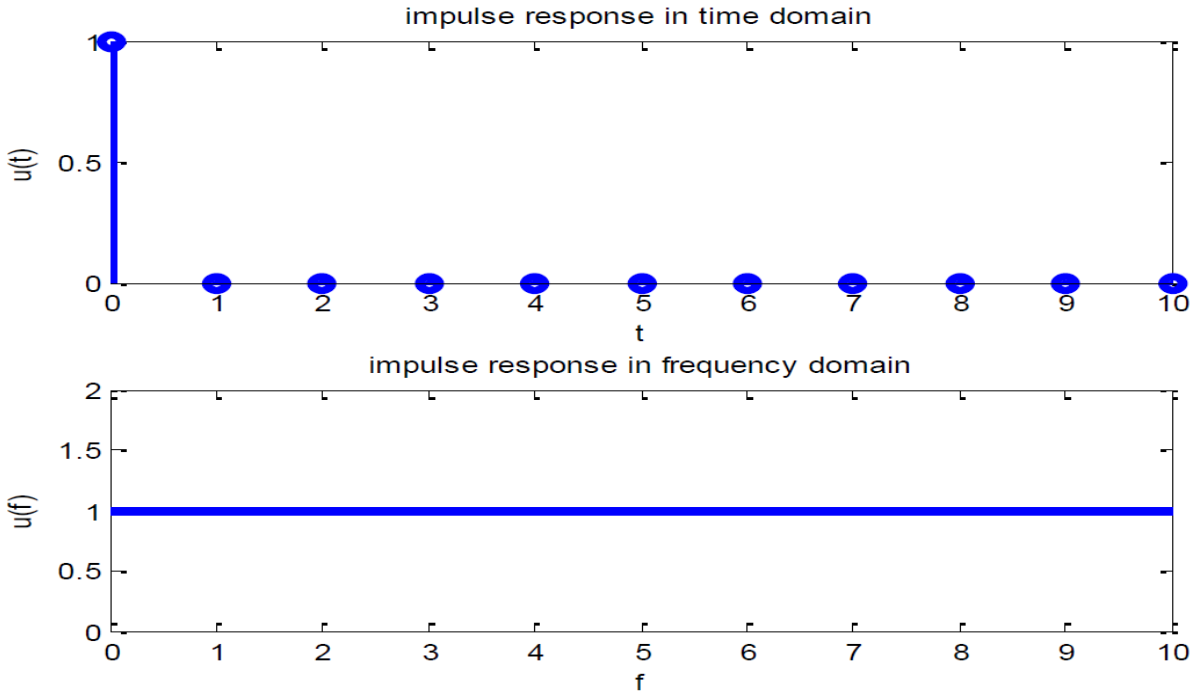

Fig. 4.7. Time-domain and frequency-domain response of impulsive noise.

One component is the additive white Gaussian noise with variance σ_n^2 and another is a high variance (σ_i^2) Gaussian component which lasts only for a short duration of symbol period, μ [11]-[13]. The total power (σ_t^2) of gated Gaussian impulse noise can be expressed as

$$\sigma_t^2 = \mu\sigma_i^2 + \sigma_n^2 \qquad (4.15)$$

This model accurately characterizes the impulse noise and helps in simulation environments as the power and the length of impulsive noise can be easily controlled and its effects on the system can be accurately analyzed. This model is used in digital video broadcasting systems to characterize the impulsive noise in the channel [11], [13].

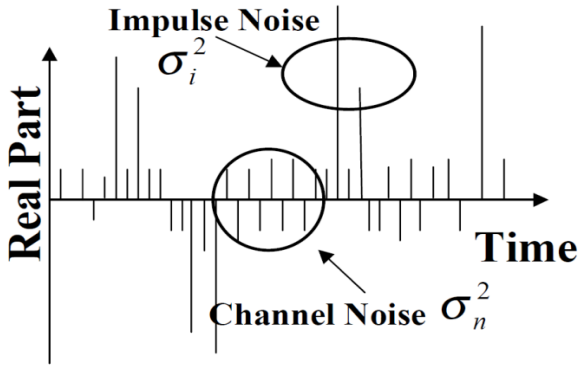

Fig. 4.8. Gated Gaussian model for impulsive noise [11].

4.5 Mitigation Techniques

4.5.1 Variance Based Peak Detection Method – ZKV Method

In [14], Zhidkov proposed a new algorithm (ZKV Method) for impulsive noise estimation and mitigation in frequency-domain after demodulation and equalization of the OFDM signal that has been adopted for digital video broadcasting. This method can be explained by the block diagram in Fig. 4.8. The peak detector in the Fig. 4.8 does the function described by Eq. (4.19) and Eq. (4.20).

It is assumed that the receiver has perfect channel estimation $\left(\hat{H}_k = H_k\right)$. The frequency-domain equalization process is called the demapping and pilot insertion procedure and is done by the following steps:

1. Replacing the silent subcarriers with zeroes
2. Replacing the known values for pilot subcarriers
3. Demapping the transmitted data on the constellation diagram to the nearest point.

The received signal converted to frequency-domain consists of transmitted signal, X_k, affected by channel response, H_k, added with AWGN, W_k, and impulsive noise, I_k, expressed as

$$R_k = H_k X_k + W_k + I_k \qquad for\ 0 \le k \le N-1 \tag{4.16}$$

The output of the equalization process is expressed as

$$R_k^{eq} = R_k \hat{H}_k^{-1} = X_k + W_k \hat{H}_k^{-1} + I_k \hat{H}_k^{-1} \qquad for\ 0 \le k \le N-1 \tag{4.17}$$

Following the frequency-domain equalization process, the total noise component is estimated as

$$\hat{Y}_k = \hat{H}_k \left(R_k^{eq} - X_k \right) \qquad for\ 0 \le k \le N-1 \tag{4.18}$$

This total noise component contains both the noises: AWGN and impulsive noise. The estimation process for the impulsive noise follows the following steps:

1. First the total noise component is converted to time-domain by using IDFT to obtain $\hat{y}_m, 0 \le m \le N-1$.
2. The variance of this time-domain noise component is evaluated to obtain an estimation of the power of the noises present and is estimated by

$$\hat{\sigma}^2 = \frac{1}{N} \sum_{m=0}^{N-1} |\hat{y}_m|^2 \tag{4.19}$$

3. The impulsive noise is estimated as using the rule

$$\hat{i}_m = \begin{cases} \hat{y}_m & if\ |\hat{y}_m|^2 > C\hat{\sigma}^2 \\ 0 & otherwise \end{cases} \qquad for\ 0 \le k \le N-1 \tag{4.20}$$

where, C is the threshold value that is used to correspond to the small probability of false detection.

4. This time-domain impulsive noise is converted to frequency-domain impulsive noise, $\hat{I}_k$, using DFT and then multiplied by the inverse channel response and then subtracted from the output of the equalizer to obtain

$$R_k^{comp} = R_k^{eq} - \hat{I}_k \hat{H}_k^{-1} \qquad for\ 0 \le k \le N-1 \tag{4.21}$$

This is the received signal after removing the impulsive noise from the received signal.

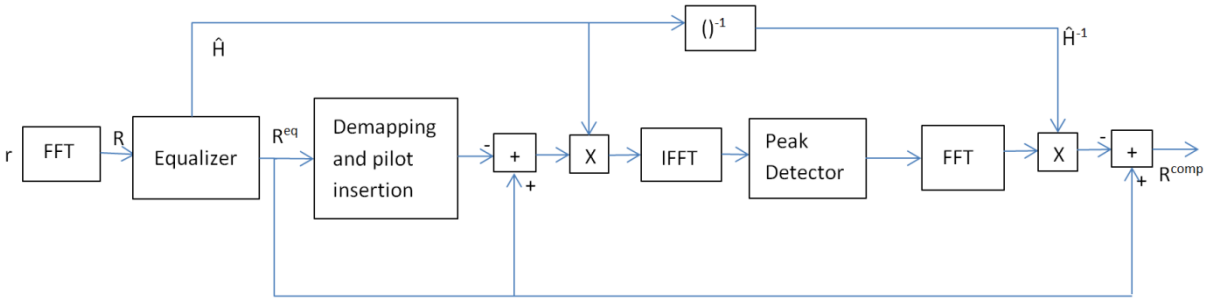

Fig. 4.9. Block diagram illustrating the ZKV method [14].

4.5.2 Modified Mean Replacement Method – CCV Method

In [15], authors have proposed a new method to mitigate the impulsive noise from the received signal. They have used a modified mean windowing filter to estimate the impulsive noise and then remove it from the received signal as opposed to replacing the OFDM signal with the mean values as is done in the conventional mean filters. This proposed method is illustrated in Fig. 4.9.

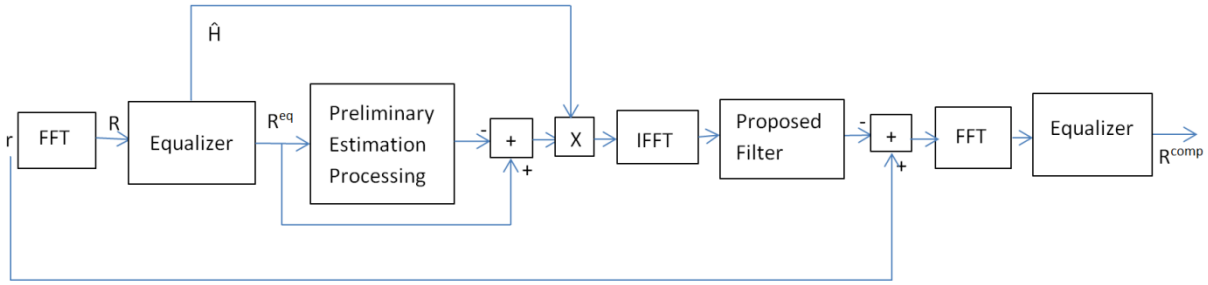

Fig. 4.10. Block diagram illustrating the CCV method [15].

The equalization process in this method is same as described in ZKV method in (4.16)-(4.18)

The composite-comparison-value (CCV) for modified mean windowing filter is evaluated as

1. First the total noise component is converted to time-domain by using IDFT to obtain $\hat{y}_m \ \ for\ 0 \le m \le N-1$.

2. The estimated noise is then sampled randomly at sampling rate to obtain sequence $s_m \ \ for\ 0 \le m \le M-1$ which is a subset of the estimated noise.

3. Windowing in now applied to the sampled sequence to obtain v_m. Each window is of size $2D+1$ such that the center element is the sampled value with D elements from each side of the sampled value is taken in the window. CCV λ_m is evaluated as

$$\lambda_m = \frac{\max|v_m| - \min|v_m|}{mean|v_m|} \tag{4.22}$$

where, max denoted the maximum value, min denotes the minimum value, mean denotes the mean value and || is used to obtain the absolute value.

4. This process is applied on all the elements of the sampled elements and the mean value is evaluated as

$$\bar{\lambda} = \frac{\sum_{m=0}^{M-1} \lambda_m}{M} \tag{4.23}$$

5. Now the windowing is applied to every estimated noise element to obtain the CCV $\dot{\lambda}_m$ as

$$\dot{\lambda}_m = \frac{|\hat{y}_m| - \min|\dot{v}_m|}{mean|\dot{v}_m|} \qquad for\ 0 \le m \le N-1 \tag{4.24}$$

The proposed method for impulsive noise estimation is explained as

1. First the absolute value of the noise that is the center of the current window, is compared to the mean of the sampling sequence as

$$|\hat{y}_m| \ge mean|s| \tag{4.25}$$

If the condition is satisfied then the process continues otherwise the filtering process stops and processing continues for the next element.

2. The impulsive noise is estimated as

$$\hat{i}_m = \begin{cases} \hat{y}_m & if\ \dot{\lambda}_m \ge \bar{\lambda} \\ 0 & otherwise \end{cases} \tag{4.26}$$

This impulsive noise classifies the signal at the center of the window as either impulsive or not.

3. The impulsive noise is then removed as

$$\tilde{r}_m = r_m - \hat{i}_m \tag{4.27}$$

This is the signal without the impulsive noise. This signal is then converted to frequency-domain and then equalized.

$$\tilde{R}_k^{eq} = \tilde{R}_k \hat{H}_k^{-1} \tag{4.28}$$

This is the final output of the CCV scheme after removing the impulsive noise component from the received signal.

Chapter 5

OPTIMIZATION OF PARAMETERS FOR IMPULSIVE NOISE MITIGATION METHODS

This chapter discusses the model used for OFDM system in impulsive noise environment. Further, the error introduced in imperfect channel estimation process has been discussed. The performance of conventional OFDM system, ZKV-OFDM system and CCV-ODFM system are analysed under perfect CSI and imperfect CSI while optimizing the parameters used in the impulsive noise mitigation schemes discussed in the previous chapter.

5.1 Introduction

For high data rate communication systems, OFDM is being widely utilized [4]. Many modern applications like terrestrial-digital-video-broadcasting (DVB-T) utilize OFDM system. The main advantages, that OFDM provides, are its robustness against impulsive noise and multipath distortions. OFDM systems used in urban environments face an additional challenge of man-made noise. Man-made noise is the main source for generating impulsive noise [6]. The source of impulsive noise varies from power lines to vehicular ignition to keyboard click. When this impulsive noise is weak, the long symbol period can mitigate its severe effects. This is due to the spreading effect because of the DFT operation performed at the receiver. The energy of the impulsive noise is spread across the symbol. But in cases when the energy of the impulsive noise is high, the advantage of DFT turns into disadvantage. To effectively suppress the impulsive noise in OFDM system, the origin, nature and source is very essential [46], [47], [29].

Though the OFDM system has inherent robustness to the effects of impulsive noise, but to improve the system performance in conditions with high impulsive noise, different schemes are incorporated to the OFDM system. Two such schemes have been discussed in the previous chapter. These schemes are implemented following the equalisation of the received signal in frequency-domain. Both these schemes have assumed perfect CSI at the receiver but practically, even with both linear and nonlinear adaptive filtering techniques, some error is inevitable in channel estimation.

This study aims to optimize the parameters used in the schemes proposed by the authors in [14] and [15] and study their performance with imperfect CSI.

5.2 OFDM System Model and Impulsive Noise Channel

This section discusses the model for the OFDM system used for simulating the transmitter and receiver in the presence of impulsive noise. Fig. 5.1 shows the block diagram illustrating the transmission and reception scheme used.

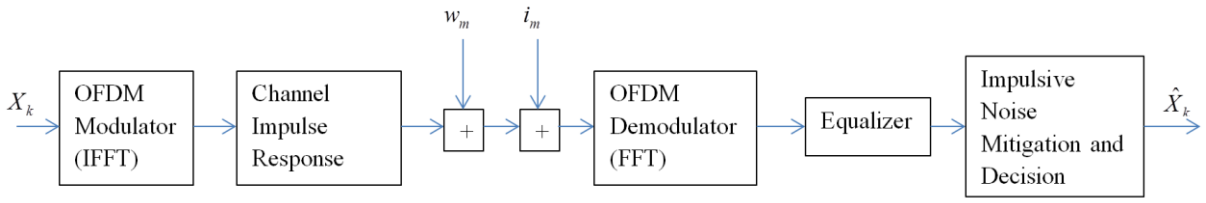

Fig. 5.1. Block diagram for transmission and reception schemes used.

At the transmitter, the data is first encoded using a suitable modulation scheme like QPSK, 16-QAM or 64-QAM. This maps the input bits to a constellation diagram to generate a complex stream of symbols $\{X_k\}$. This work uses 16-QAM to simulate all the conditions used, so the modulator takes in four information bits and provides the output representing any of the points from the constellation diagram. X_k is now fed to the IFFT block to obtain x_m which is time-domain signal. The complex baseband OFDM signal is expressed as

$$x_m = \frac{1}{\sqrt{N}} \sum_{k=0}^{N-1} X_k \exp\left(\frac{j2\pi Bm}{N}\right) \qquad for\ 0 \le m \le T_m \tag{5.1}$$

where, B denotes the total bandwidth of the OFDM symbol, N is the number of subcarriers used in each OFDM symbol and T_m is the time interval for the OFDM symbol.

The frequency separation between two consecutive OFDM symbols can be donated by Δf expressed as

$$\Delta f = \frac{B}{N} \tag{5.2}$$

The output of the IFFT block can be expressed as

$$x_m = \frac{1}{\sqrt{N}} \sum_{k=0}^{N-1} X_k \exp\left(j2\pi\Delta fm\right) \qquad for\ 0 \le m \le N-1 \tag{5.3}$$

At the receiver, the signal obtained after conversion from analog-to-digital domain can be expressed as

$$r_m = z_m + w_m + i_m \tag{5.4}$$

where, z_m, w_m, i_m are assumed to be mutually independent to each other. w_m denotes the AWGN added in the channel, i_m denotes the impulsive noise added in the channel from variable man-made sources and z_m is expressed as

$$z_m = \sum_{l=1}^{L} h_l x_{m-l} \tag{5.5}$$

where, h_l is the impulse response of the channel, L is the length of the impulse response of the channel and x_m can be expressed as

$$x_m = x\left(\frac{mT_m}{N}\right) \tag{5.6}$$

The received signal can be expressed as

$$r_m = \sum_{l=1}^{L} h_l x_{m-l} + w_m + i_m \qquad for\ 0 \le m \le N-1 \tag{5.7}$$

This received signal is complex in nature and all the constituents are also assumed to be complex including AWGN and impulsive noise. The impulsive noise has been modelled by gated Gaussian model. This denotes the impulsive noise as the sum of AWGN and a high variance Gaussian noise, which lasts only for a short duration of time. The received signal is converted to frequency-domain by performing FFT operation to obtain the received signal as

$$R_k = H_k X_k + W_k + I_k \tag{5.8}$$

where, $H = \left[H_0, H_1, H_2, \cdots, H_{N-1}\right]$ denotes the frequency-domain impulsive channel response, $X = \left[X_0, X_1, X_2, \cdots, \mathrm{X}_{N-1}\right]$ is the frequency-domain transmitted signal and the frequency-domain AWGN can be written as $W = \left[W_0, W_1, W_2, \cdots, \mathrm{W}_{N-1}\right]$. The frequency-domain impulsive nose can be expressed as $I = \left[I_0, I_1, I_2, \cdots, \mathrm{I}_{N-1}\right]$.

5.3 Mathematical Model for Imperfect CSI for Impulsive Noise Mitigation

The methods that were employed in earlier OFDM systems used impulsive noise mitigation techniques in time-domain. The methods discussed in the previous chapter are implemented in frequency-domain after the demodulation process with perfect channel-state-information (CSI).

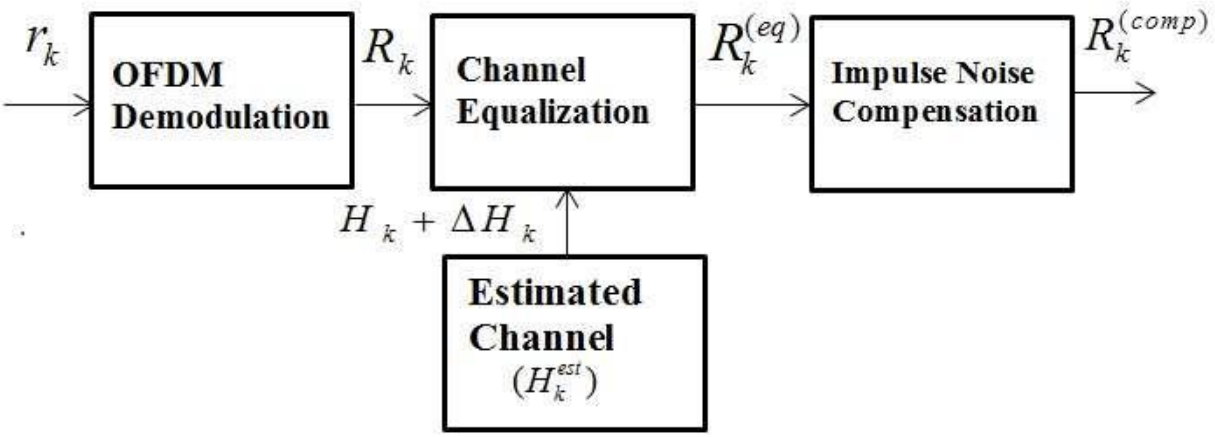

Fig. 5.2. Reception of signal with imperfect channel state information.

However, in practical systems, the receiver does not have perfect knowledge of the channel state. The imperfections in the channel estimation process is mainly caused by estimation errors of the channel and/or by channel variations die to motion of either the transmitter or receiver or both [50]. In both linear and nonlinear adaptive channel estimation techniques [48]-[49], the channel estimation error is inevitable. Thus, the receiver has channel parameter as H_k^{est}, which is equal to the sum of perfect channel state information and estimation error i.e. $H_k^{est} = H_k + \Delta H_k$.

As in [16], the authors have obtained the error in estimation process in symbol detection as follows.

The equalised signal obtained after using estimated CSI can be expressed as

$$R_k^{(eq)} = R_k \left(H_k^{est}\right)^{-1} = H_k X_k \left(H_k^{est}\right)^{-1} + W_k \left(H_k^{est}\right)^{-1} + I_k \left(H_k^{est}\right)^{-1} \qquad for\ 0 \le k \le N-1 \quad (5.9)$$

where, the error in the estimation of the channel state information is ΔH_k. It is a complex number represented as $\Delta H_k = a_k + jb_k$. Here, a_k and b_k are random variables, which are independent and identical with Gaussian distribution with zero mean and variance $\sigma_k^2/2$.

$$R_k\left(H_k+\Delta H_k\right)^{-1}=H_kX_k\left(H_k+\Delta H_k\right)^{-1}+W_k\left(H_k+\Delta H_k\right)^{-1}+I_k\left(H_k+\Delta H_k\right)^{-1} \tag{5.10}$$

Taking the term ΔH_k^{-1} common from both sides of the equation leads to

$$R_kH_k^{-1}\left(1+\frac{\Delta H_k}{H_k}\right)^{-1}=X_k\left(1+\frac{\Delta H_k}{H_k}\right)^{-1}+W_kH_k^{-1}\left(1+\frac{\Delta H_k}{H_k}\right)^{-1}+I_kH_k^{-1}\left(1+\frac{\Delta H_k}{H_k}\right)^{-1} \tag{5.11}$$

Using Taylor series expansion $\left(i.e.\left(1+x\right)^{-1}\approx\left(1-x\right)\right)$ on this expression gives

$$R_kH_k^{-1}\left(1-\frac{\Delta H_k}{H_k}\right)=X_k\left(1-\frac{\Delta H_k}{H_k}\right)+W_kH_k^{-1}\left(1-\frac{\Delta H_k}{H_k}\right)+I_kH_k^{-1}\left(1-\frac{\Delta H_k}{H_k}\right) \tag{5.12}$$

Thus, the equalised received signal with imperfect CSI can be written as, [16]

$$R_k^{eq}=X_k\left(1-\frac{\Delta H_k}{H_k}\right)+\left(W_k+I_k\right)H_k^{-1}\left(1-\frac{\Delta H_k}{H_k}\right) \tag{5.13}$$

Let the estimated transmitted signal be $\hat{X}_k$ and the total estimated noise term in the received signal is expressed as $Y_k=W_k+I_k\ \ for\ 0\le k\le N-1$. The estimated total noise term can be expressed as

$$Y_k^{est}=\left(R_k^{eq}-\hat{X}_k\left(1-\frac{\Delta H_k}{H_k}\right)\right)H_k\left(1-\frac{\Delta H_k}{H_k}\right)^{-1} \tag{5.14}$$

$$Y_k^{est}=\left(\left(R_kH_k^{-1}-\hat{X}_k\right)H_k\left(1-\frac{\Delta H_k}{H_k}\right)\right)\left(1-\frac{\Delta H_k}{H_k}\right)^{-1} \tag{5.15}$$

By Taylor series expansion $\left(1-\frac{\Delta H_k}{H_k}\right)^{-1}\approx\left(1+\frac{\Delta H_k}{H_k}\right)$, substituting and reducing the equation to

$$Y_k^{est}=\left(R_kH_k^{-1}-\hat{X}_k\right)H_k\left(1-\left(\frac{\Delta H_k}{H_k}\right)^2\right) \tag{5.16}$$

But $\left(R_kH_k^{-1}-\hat{X}_k\right)H_k=W_k+I_k$. Replacing the above equation

$$Y_k^{est}=\left(W_k+I_k\right)\left(1-\left(\frac{\Delta H_k}{H_k}\right)^2\right) \tag{5.17}$$

$$Y_k^{est}=Y_k+\varepsilon \tag{5.18}$$

The estimated noise vector $\vec{Y}=\left[Y_0,Y_1,...,\mathrm{Y}_{N-1}\right]$ is the total noise component in the received signal. This noise term is in the frequency-domain containing both impulsive noise

and AWGN. The error in the noise term is represented as ε. This is the error introduced due to imperfect CSI at the receiver. The impulsive noise in frequency-domain can be represented as the sum of complex sinusoids

$$I_k = A_1 e^{j2\pi k l_1/N} + A_2 e^{j2\pi k l_2/N} + ... + A_M e^{j2\pi k l_M/N} \quad (5.19)$$

where, M is the total number of samples that are affected by the impulsive noise, the locations of these samples are denoted by $I_1, I_2, I_3, \cdots, I_M$. The amplitudes of the impulsive interference is denoted by $A_1, A_2, A_3, \cdots, A_M$. The impulsive noise mitigation methods, discussed in the last chapter, aim to find the locations of these impulsive samples and determine their amplitudes. Using this information, the impulsive noise component is reconstructed and removed from the received signal. The impulsive noise component is removed from the received signal in either time-domain or frequency-domain depending on the method employed.

The performance of the system can be improved by applying these methods recursively. For high amplitude impulsive noise, it is preferred to remove the impulsive noise using time-domain compensation methods like blanking nonlinearity before proceeding to demodulation process. The next section discusses the simulation results of the two methods discussed in the last chapter under perfect CSI and imperfect CSI conditions to find out the optimum parameters for applying the methods.

5.4 Simulation Result

In this section, we will investigate the bit-error-rate (BER) performance of OFDM system (using impulsive noise mitigation techniques) working under the Rayleigh fading environment [50], which is corrupted by impulsive noise as well as AWGN. Though the channel is frequency-selective in nature, but it appears to be flat fading while using OFDM technology [27]. The parameters in different impulsive noise mitigation techniques are varied to identify the optimum values like threshold value for ZKV scheme and window size for CCV scheme. The impulsive noise statistics changes with the number of impulses encountered by an OFDM system under different fading conditions [12]. The number of subcarriers is considered to be 256.

The main goal of simulation is to evaluate the performance of underlying system under imperfect CSI. The presented results are based on the ensemble average of 1000 independent experiments. In simulation, H_{avg} is the average value of a channel tap-coefficient in frequency-domain. Here, $H_{avg} = 1$ indicates no fading. However, channel estimation error is assumed to exhibit zero-mean and variance $10\log_{10}\left(\sigma_{\Delta H}^2\right) dB$.

5.4.1 Performance of OFDM System with Mitigation Methods Under Perfect CSI

- **Case 1: Analysis with Different Values for Parameter C for ZKV Method**

In this simulation, we investigate the impact of changing value of parameter C on the performance of ZKV-OFDM system using 16-QAM in the presence of 10% impulses during a symbol period, at different values of signal-to-noise-ratio (SNR). The average value of a channel tap-coefficient in frequency-domain is kept 0.75. For comparison, the window size is considered to be 15 in CCV scheme.

Simulation results in Fig. 5.3 to Fig. 5.5 depict that as the value of C decreases the BER performance of ZKV-OFDM system improves due to reduction in probability of false detection. In the presented case, $C = 0.25$ provides the best results. However, CCV-OFDM system still performs better. Similar results are obtained in all the sizes of the OFDM symbol used. The effect of impulsive noise spreads across the entire symbol due to noise bucket effect. Due to strong impulsive noise, the advantage of spreading turns to disadvantage as more bits are corrupted in the symbol with larger size [12].

- **Case 2: Analysis with Different Fading Conditions**

Subsequently, the fading conditions are varied by changing the average value of a channel tap-coefficient in frequency-domain $H_{avg} = \{0.5, 0.75, 1\}$; while using 16-QAM modulation scheme. The number of impulses is considered to be 10% in a symbol period, N. In ZKV scheme, the threshold value is set by keeping $C = 0.25$. In CCV scheme, the window size is fixed at 15.

Table 5.1. System parameters for different threshold levels of ZKV method under perfect CSI.

Parameter	**Value**
Modulation used	16-QAM
Number of subcarriers	64, 256, 1024
Number of impulses	10% of the symbol period, N
Average value for a single channel-tap coefficient $\left(H_{avg}\right)$	0.75
Parameter C for ZKV method	0.25, 0.5, 0.75, 1, 1.5, 2, 2.5, 3
Window size for CCV method	15

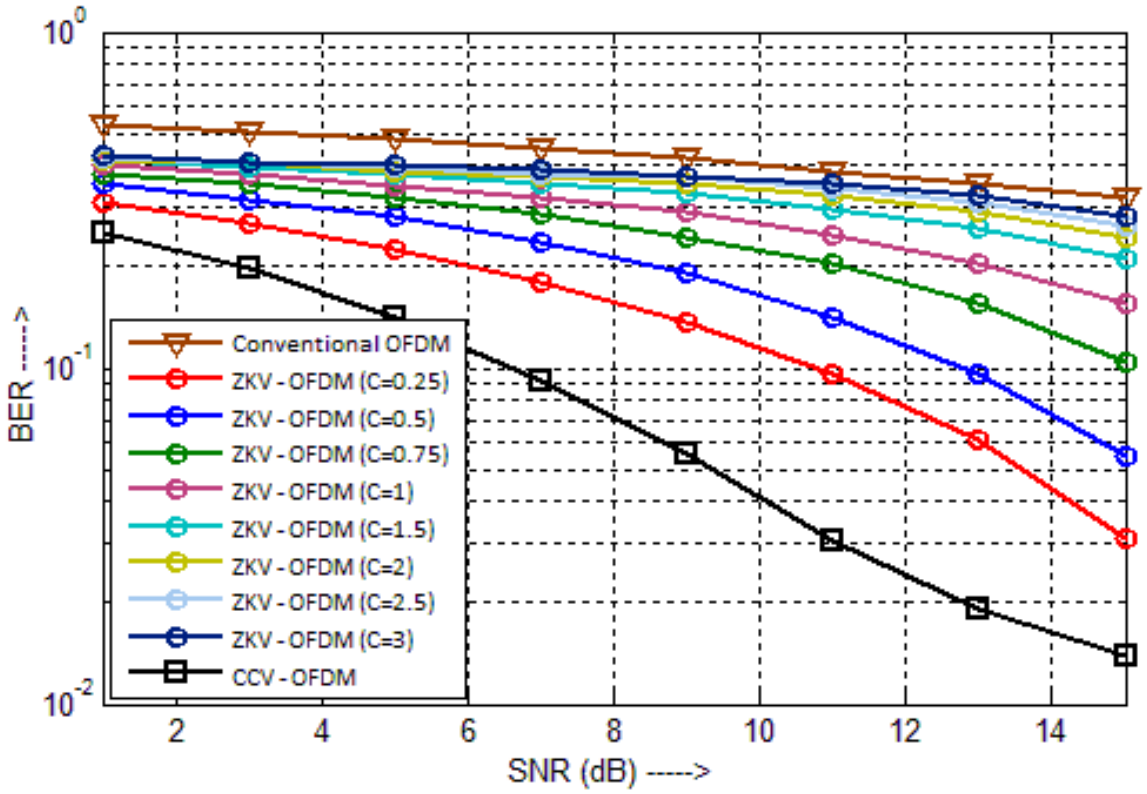

Fig. 5.3. BER vs. SNR (dB) at different values of parameter C (ZKV method) for 64 subcarriers.

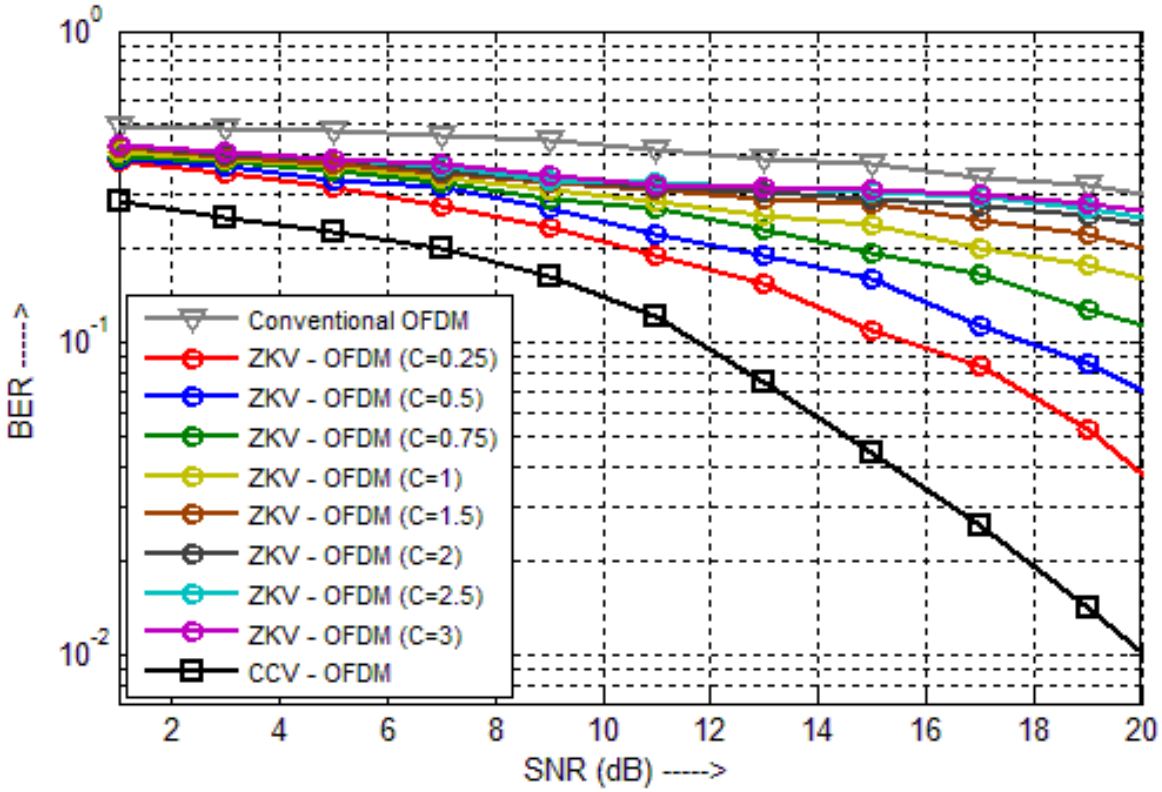

Fig. 5.4. BER vs. SNR (dB) at different values of parameter C (ZKV method) for 256 subcarriers.

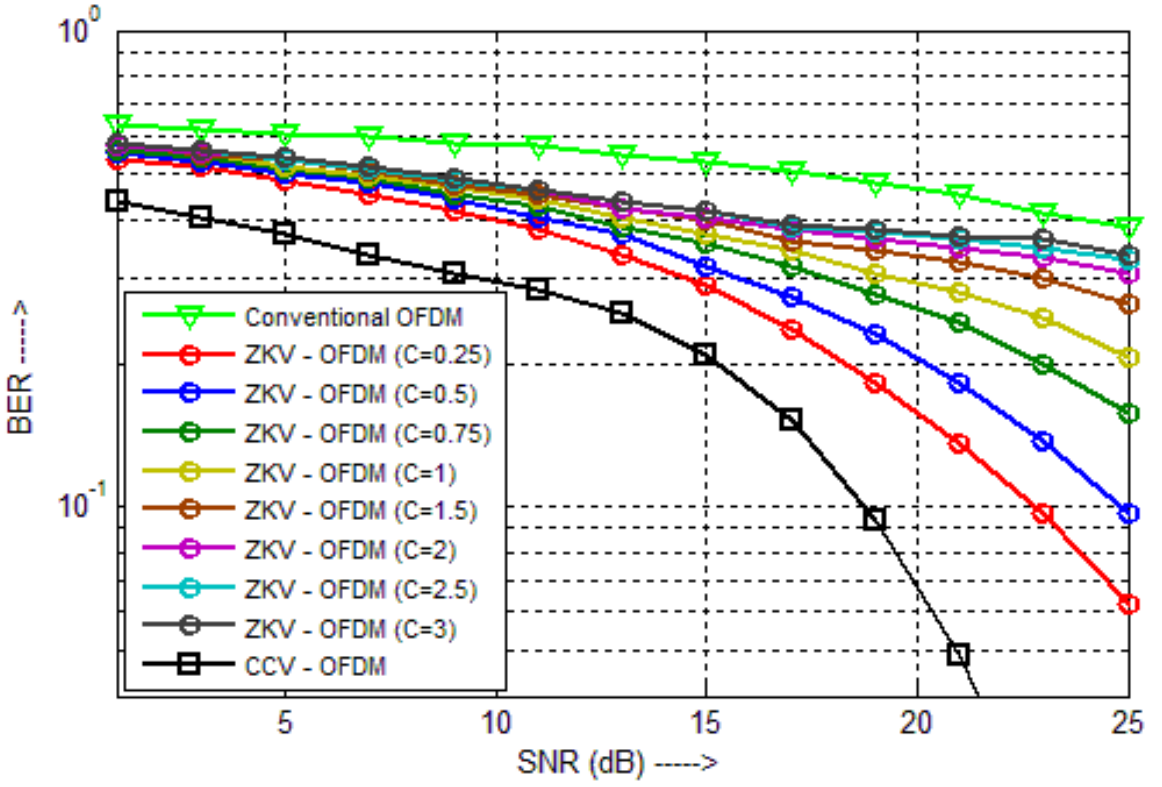

Fig. 5.5. BER vs. SNR (dB) at different values of parameter C (ZKV method) for 1024 subcarriers.

It may be inferred from Fig. 5.6 to Fig.5.8 that the BER performance of ZKV-OFDM and CCV-OFDM gets degraded with the decreasing value of H_{avg}. The case with $H_{avg} = 0.5$ represents fast fading condition in the channel. In such severe case of fading, the loss of data is high and the performance of the system is greatly affected. The case with $H_{avg} = 1$ represents no fading. This is ideal case, when the signal does not encounter any loss in its power while travelling through the channel. The performance of this condition is the best as observed in the simulation results as well. The case of $H_{avg} = 0.75$ represents average conditions of the channel. The signal is not severely degraded nor does it observe ideal conditions. The signal losses some power, but it can still provide useful information. CCV-OFDM system supersedes conventional OFDM and ZKV-OFDM systems for any value of SNR. But, its performance depends on the optimum window size, which is found through heuristic simulation. The performance follows the same pattern in all the three sizes of the OFDM symbol sizes used.

Table 5.2. System parameters for different fading conditions under perfect CSI.

Parameter	**Value**
Modulation used	16-QAM
Number of subcarriers	64, 256, 1024
Number of impulses	10% of the symbol period, N
Average value for a single channel-tap coefficient $\left(H_{avg}\right)$	0.5, 0.75, 1
Parameter C for ZKV method	0.25
Window size for CCV method	15

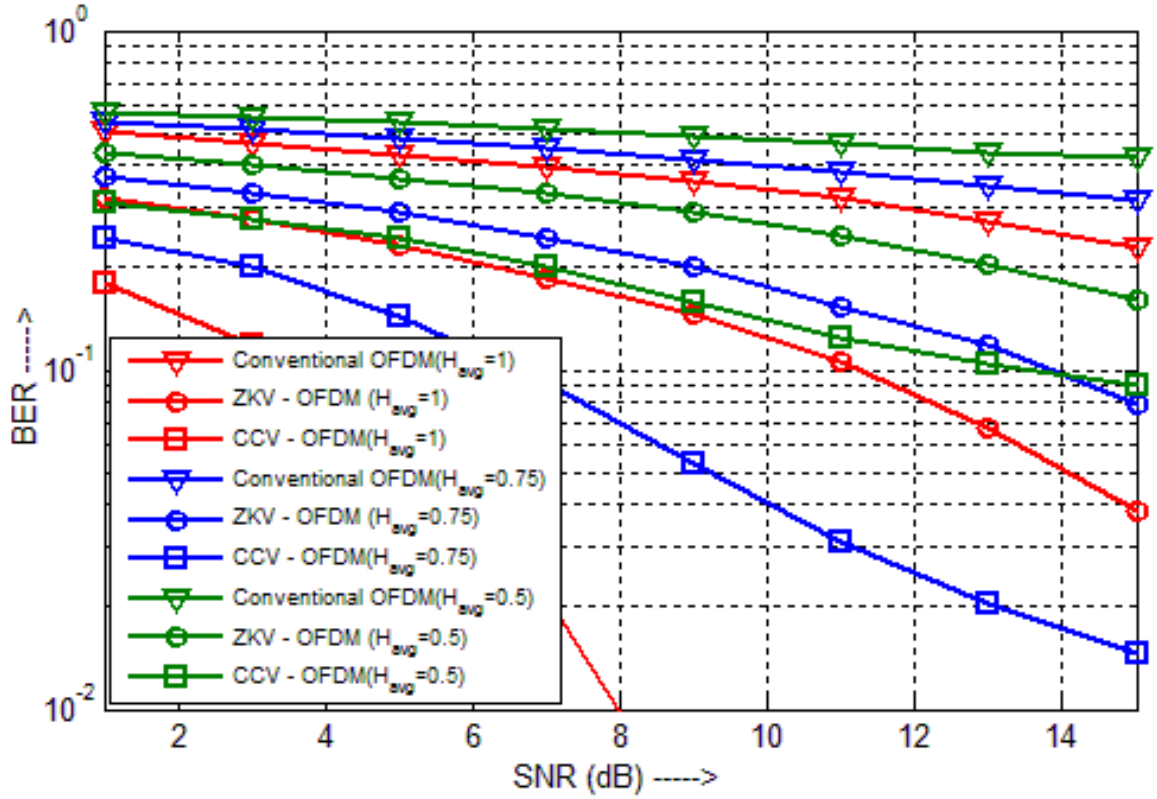

Fig. 5.6. BER vs. SNR (dB) under different fading conditions for 64 subcarriers.

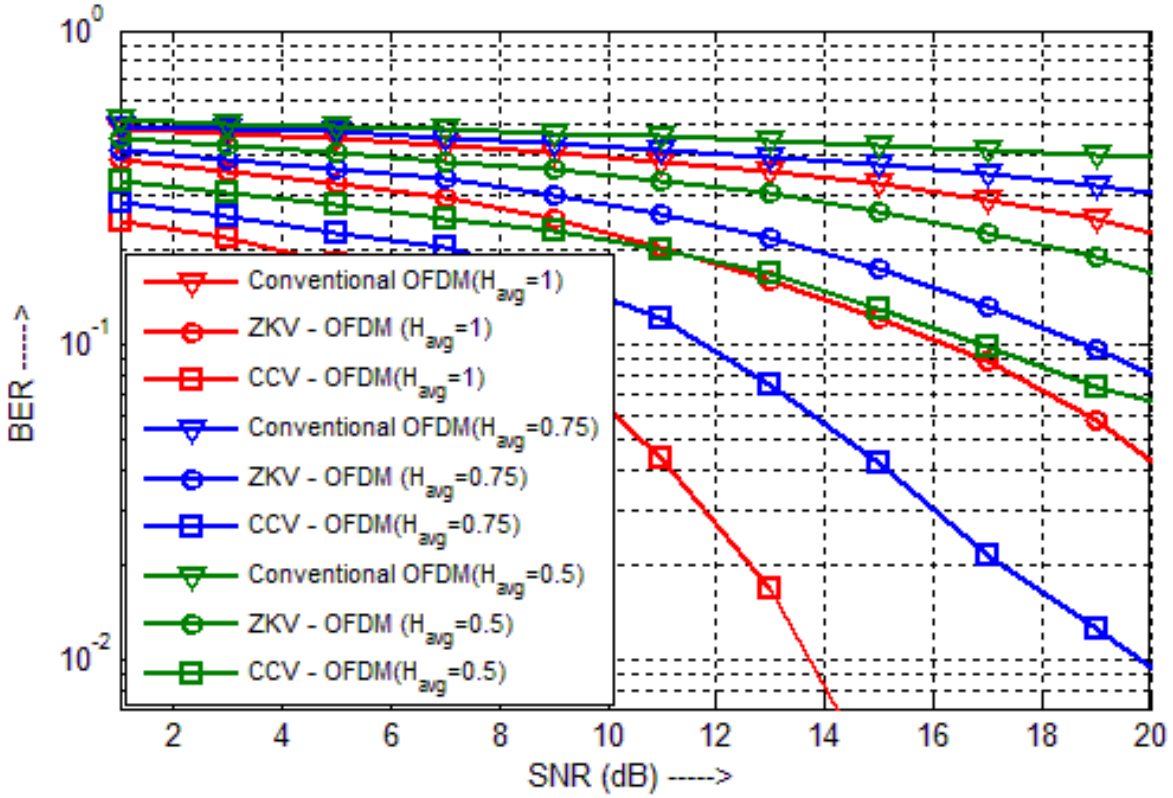

Fig. 5.7. BER vs. SNR (dB) under different fading conditions for 256 subcarriers.

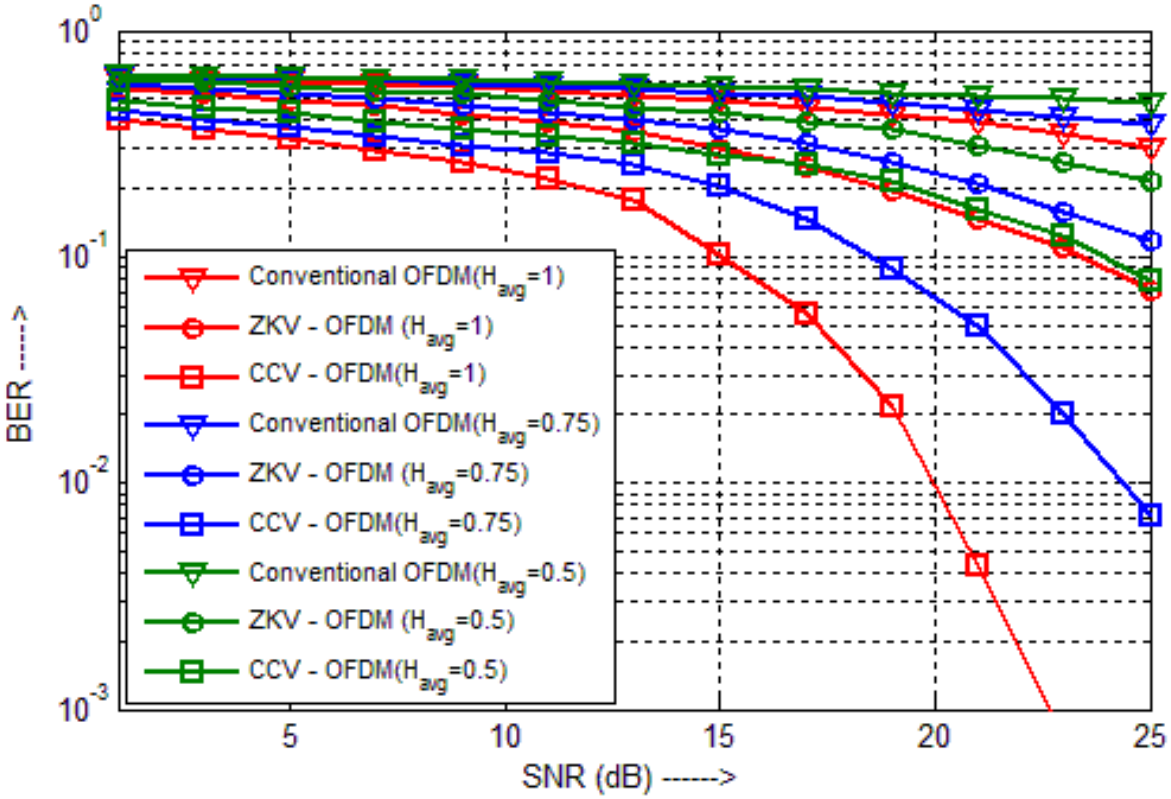

Fig. 5.8. BER vs. SNR (dB) under different fading conditions for 1024 subcarriers.

- **Case 3: Analysis with Different Number of Impulses**

The performance under different number of impulses is analysed i.e., for 5%, 10% and 15% impulses in a symbol period. The average value for the channel tap-coefficient is taken constant at 0.75 while using 16-QAM modulation scheme. The value for the parameter C for the ZKV method is taken as 0.25 and the window size for CCV method is taken as 15.

As shown in Fig. 5.9 to Fig 5.11, the performance of the OFDM system gets degraded with the increasing number of impulses in an OFDM symbol. With the increase in the number of impulses, the impulse energy spreads across the entire symbol due to spreading effect of DFT/IDFT. This noise energy introduces error in the entire symbol. It has been observed that the advantage in the system performance of CCV-OFDM is much more as the number of impulses decreases from 15% to 5% than the advantage obtained in ZKV-OFDM system and the conventional OFDM system.

Table 5.3. System parameters for different number of impulses under perfect CSI.

Parameter	**Value**
Modulation used	16-QAM
Number of subcarriers	64, 256, 1024
Number of impulses	5%, 10%, 15% of the symbol period, N
Average value for a single channel-tap coefficient $\left(H_{avg}\right)$	0.75
Parameter C for ZKV method	0.25
Window Size for CCV method	15

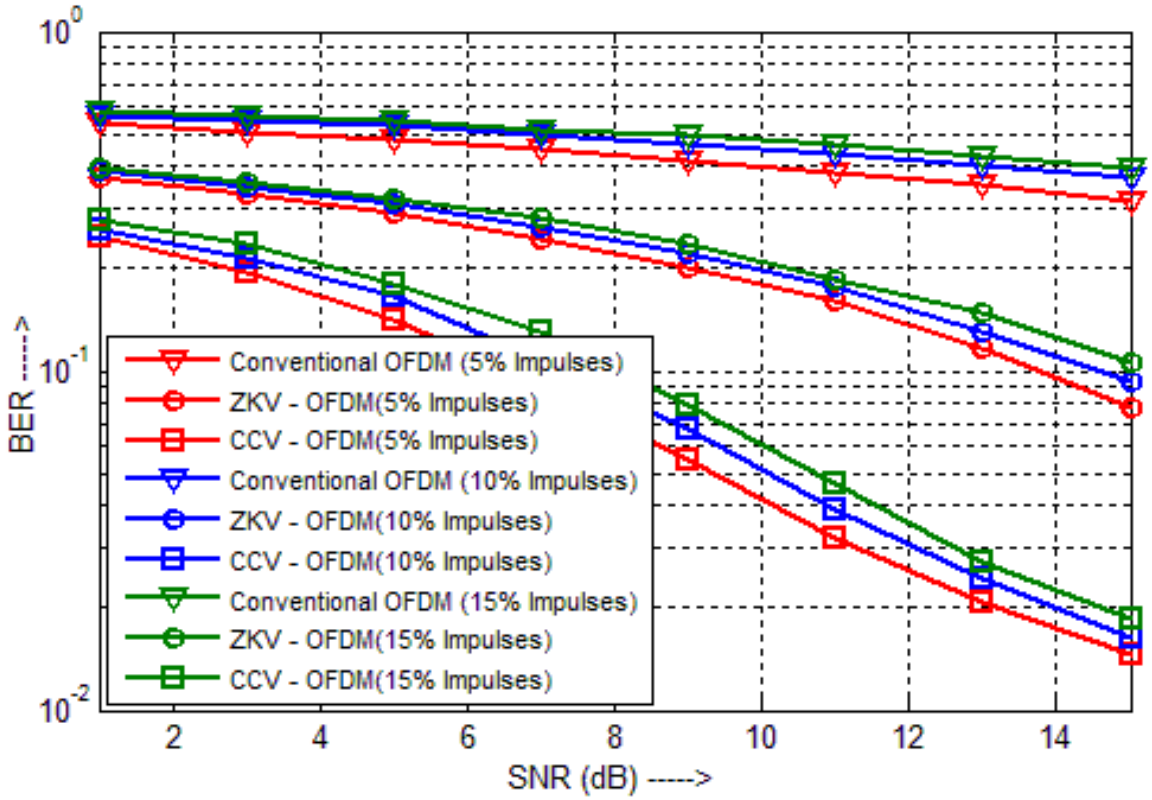

Fig. 5.9. BER vs. SNR (dB) for different number of impulses for 64 subcarriers.

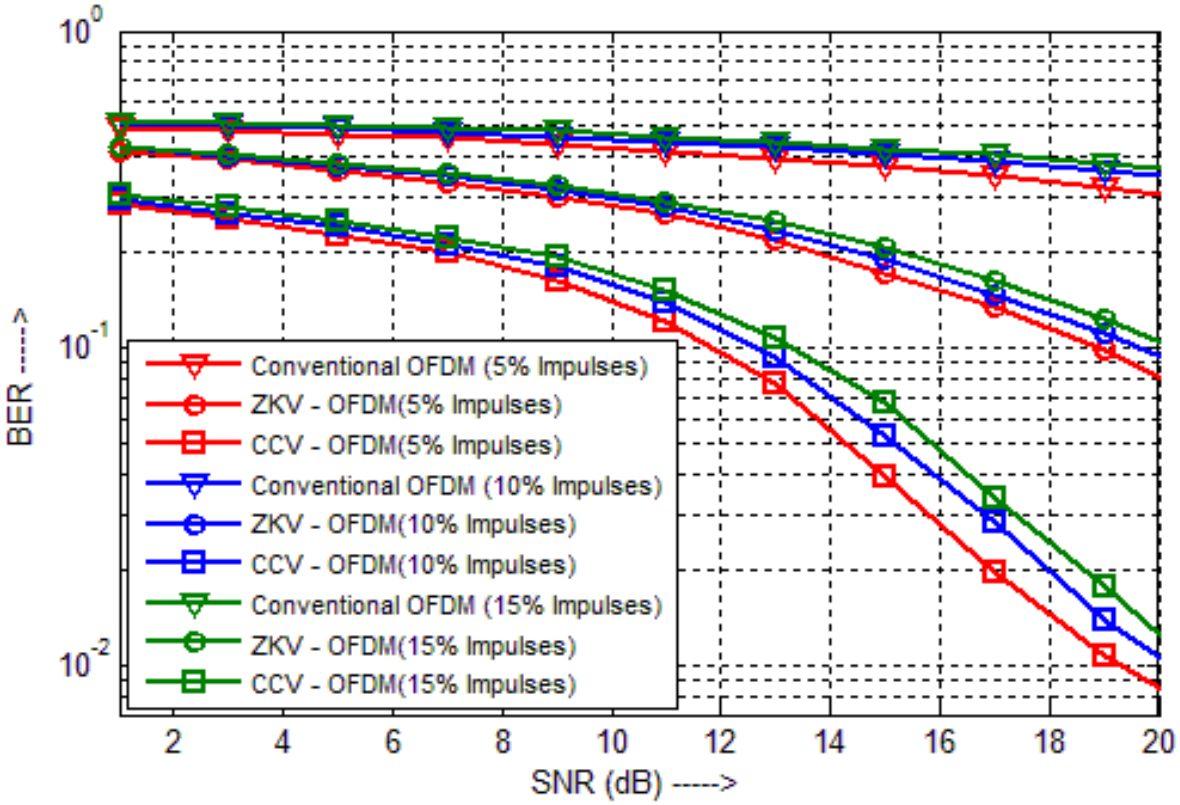

Fig. 5.10. BER vs. SNR (dB) for different number of impulses for 256 subcarriers.

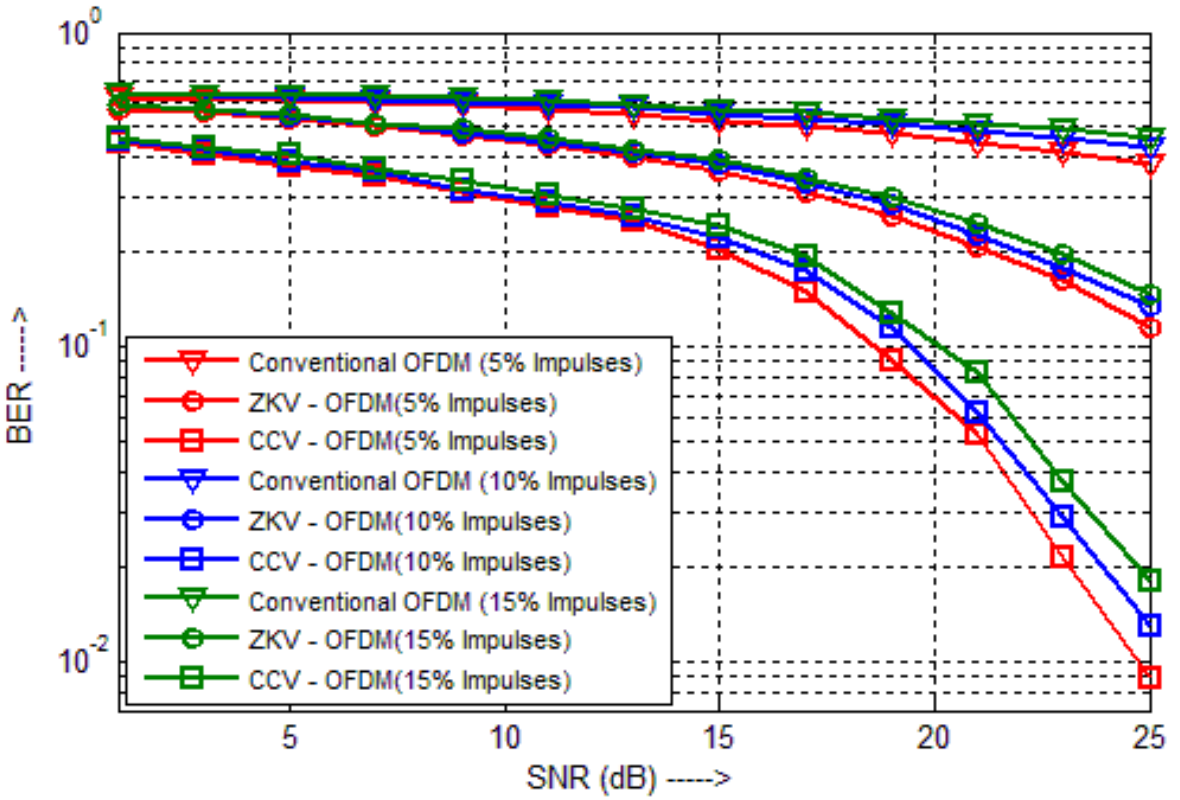

Fig. 5.11. BER vs. SNR (dB) for different number of impulses for 1024 subcarriers.

Similar observations are observed in all the three cases of different number of subcarriers. When the number of impulses is less, it add up linearly; and as their number increases it behave as Gaussian noise due to the application of central limit theorem. This can be observed when the size of OFDM increases and the number of impulses in the symbol period, N, increases from 5% to 15%. The impulsive noise behaves like Gaussian when each OFDM symbol has 1024 subcarriers and the impulsive noise has linear behaviour when the number of subcarriers is 64. This also leads to slower convergence of the system performance for the case of lesser number of subcarriers as compared to the case of 1024 subcarriers. 256 subcarriers in the OFDM symbol represent the average case.

- **Case 4: Analysis with Different Modulation Scheme**

The performance under different modulation schemes is analysed i.e., for QPSK, 16-QAM and 64-QAM. Here, 10% impulses are taken in each OFDM symbol with average value for channel tap-coefficient as 0.75. The parameter C is kept constant at 0.25 for ZKV method and the window size for CCV method is taken as 15.

As shown in Fig. 5.12 to Fig. 5.14, the performance of the OFDM system gets degraded with increase in the order of modulation scheme. This is because with higher order modulation schemes, the number of symbols used is more. With constant power of the symbols in each modulation scheme, the symbols come closer to each other, and hence the region for correct detection gets smaller. When noise is added to the symbol, there is a greater probability of wrong decoding. But as the order of modulation increases, the number of symbol increases and hence more data bits can be transmitted. This increases the data rate. So, there exists a trade-off between the data rate and error tolerance. CCV-OFDM system has outperformed the ZKV-OFDM system and the conventional system with different modulation schemes as well in all the sizes of OFDM symbol.

Table 5.4. System parameters for different modulation schemes under perfect CSI.

Parameter	**Value**
Modulation used	QPSK, 16-QAM, 64-QAM
Number of subcarriers	64, 256, 1024
Number of impulses	10% of the symbol period, N
Average value for a single channel-tap coefficient $\left(H_{avg}\right)$	0.75
Parameter C for ZKV method	0.25
Window Size for CCV method	15

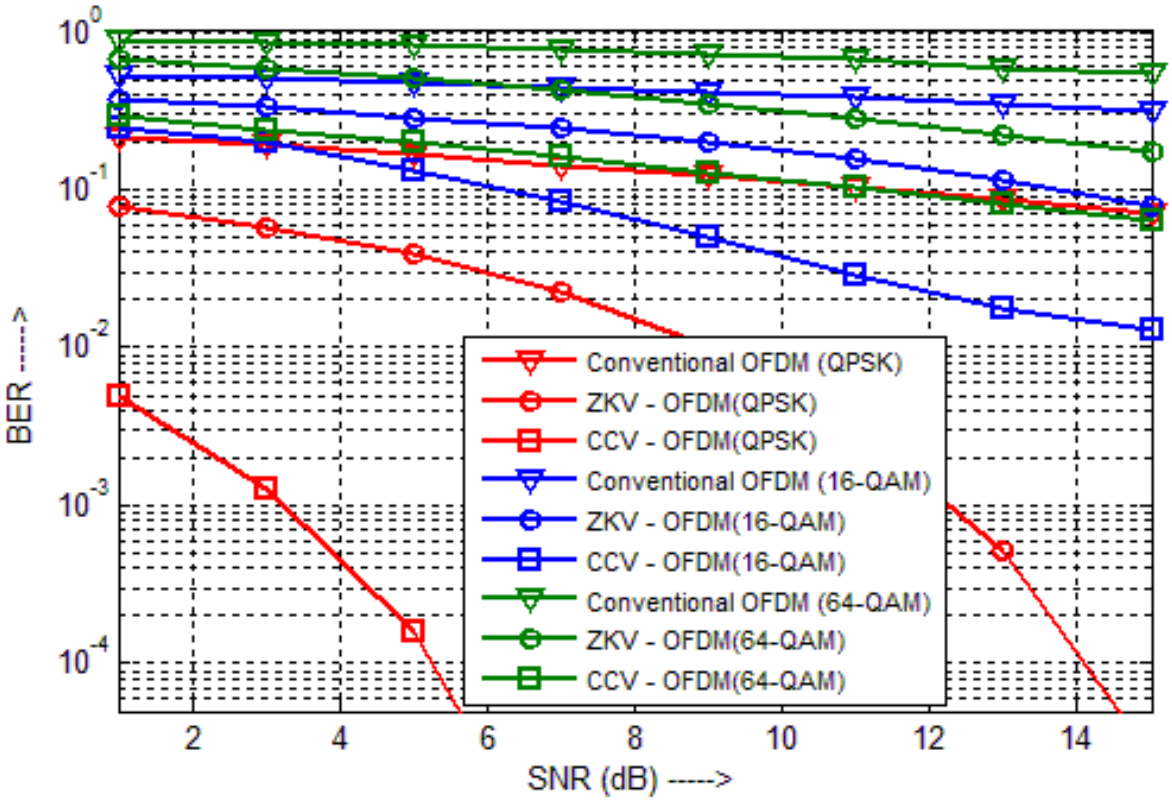

Fig. 5.12. BER vs. SNR (dB) for different modulation schemes for 64 subcarriers.

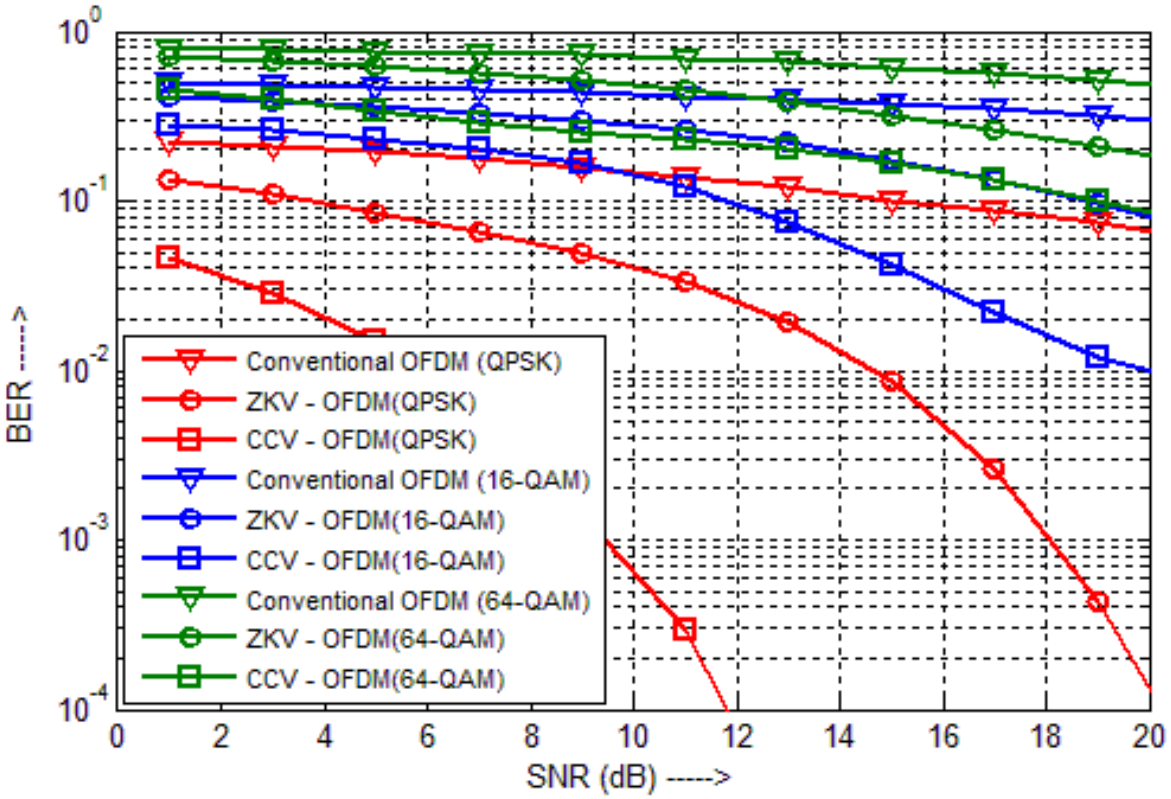

Fig. 5.13. BER vs. SNR (dB) for different modulation schemes for 256 subcarriers.

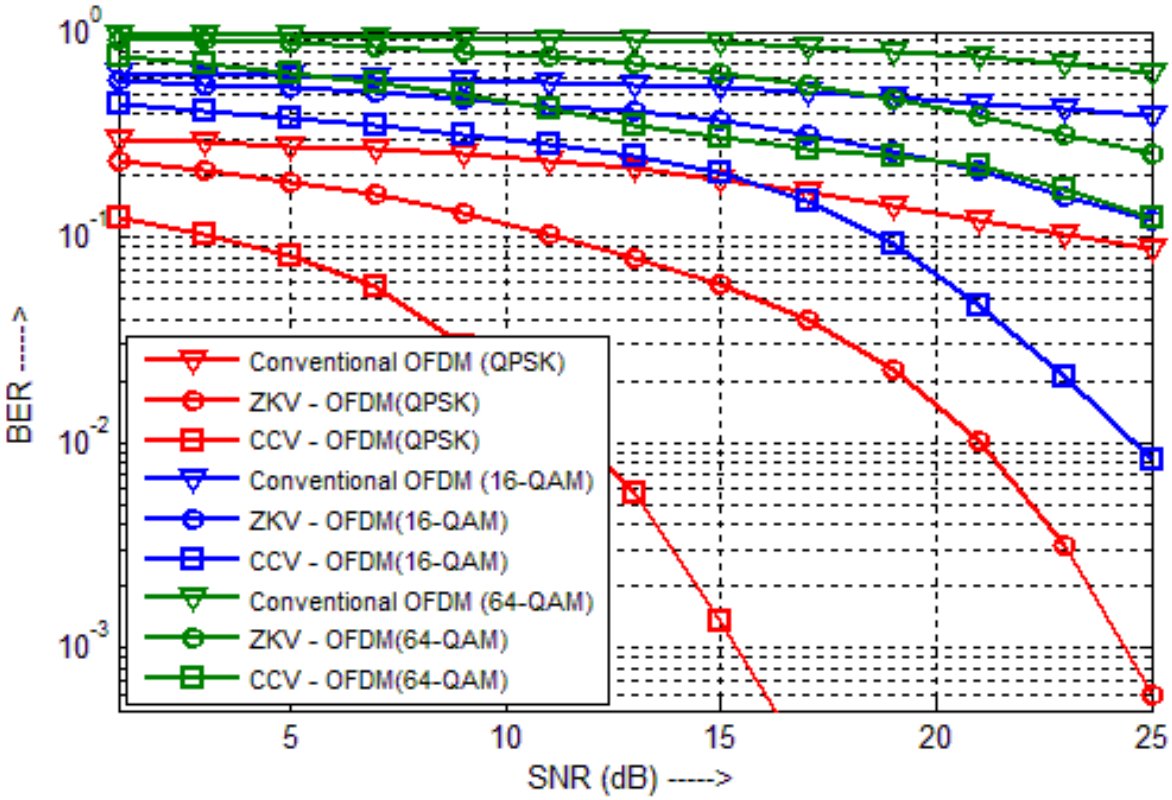

Fig. 5.14. BER vs. SNR (dB) for different modulation schemes for 1024 subcarriers.

- **Case 5: Analysis with Different Values of Window Size for CCV Method**

Further, the BER performance of CCV-OFDM system is evaluated using different value of window size in the presence of 10% impulses in a symbol period while using 16-QAM. The average value of a channel tap-coefficient in the frequency-domain is set at 0.75 and $C = 0.25$ in ZKV method. It is apparent from the simulation results demonstrated in Fig. 5.16 that at high SNR values in CCV-OFDM system, there is an advantage of approximate 1dB SNR if we reduce the window size from 25 to 15 at $BER = 0.02$. However, ZKV-OFDM system fails to perform well under similar conditions. Similar advantages have been observed in Fig. 5.15 and Fig. 5.17 for OFDM symbol sizes 64 and 1024. The advantage obtained for 1024 subcarriers is more than the advantage obtained for 256 subcarriers, which offers more advantage than the advantage for 64 subcarriers for same window size.

Table 5.5. System parameters for simulation for different window size of CCV-method under perfect CSI.

Parameter	**Value**
Modulation used	16-QAM
Number of subcarriers	64, 256, 1024
Number of impulses	10% of the symbol period, N
Average Value for a single channel-tap coefficient $\left(H_{avg}\right)$	0.75
Parameter C for ZKV method	0.25
Window Size for CCV method	5, 15, 25

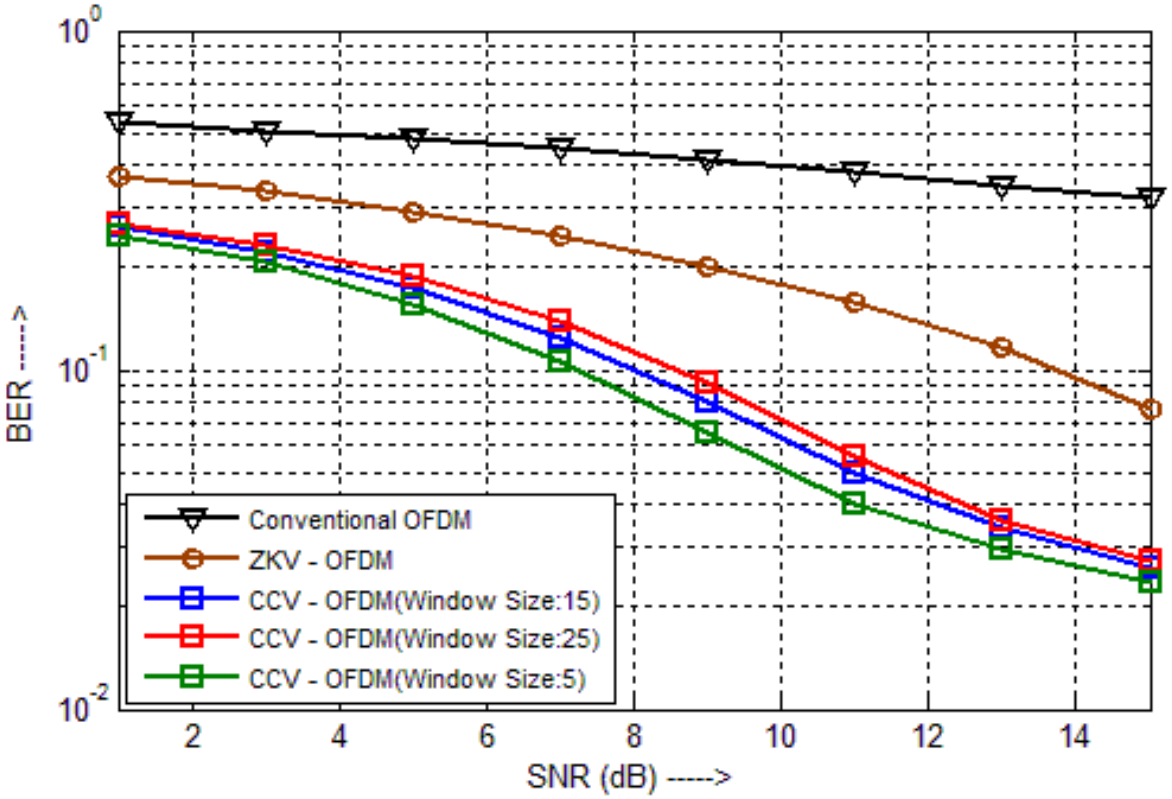

Fig. 5.15. BER vs. SNR (dB) for different window size for CCV- method with 64 subcarriers.

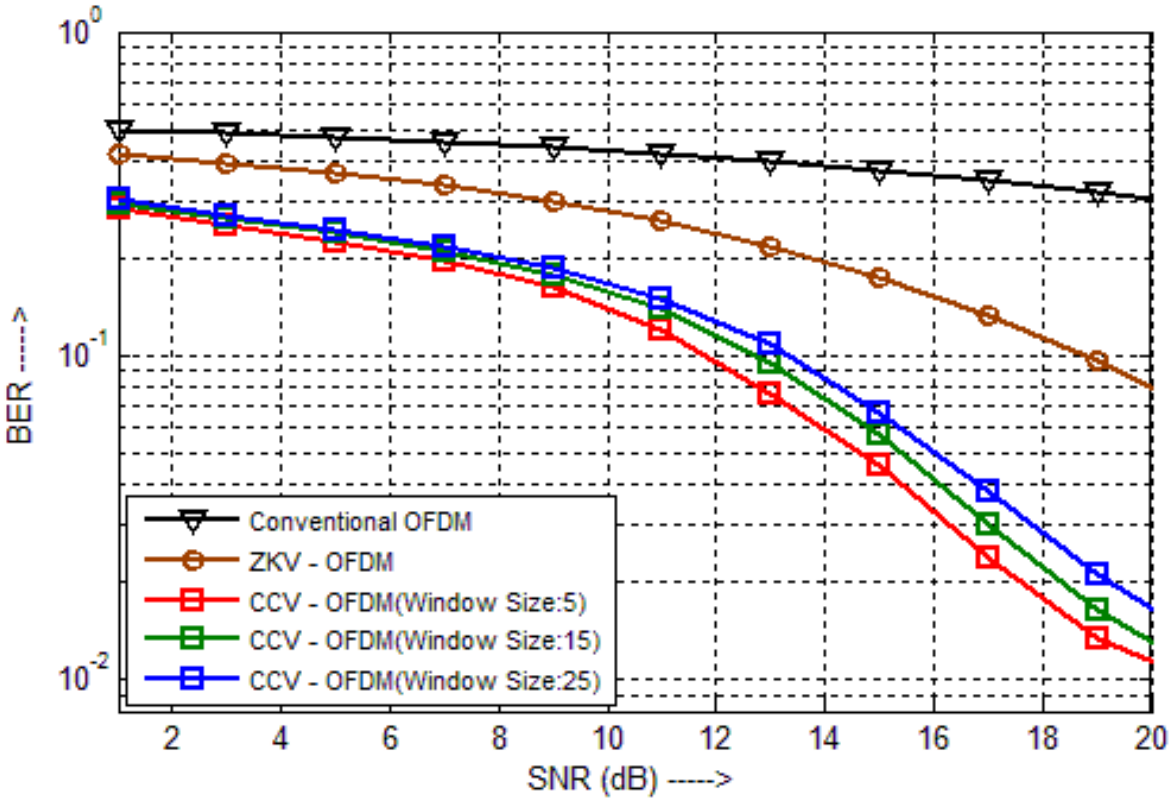

Fig. 5.16. BER vs. SNR (dB) for different window size for CCV- method with 256 subcarriers.

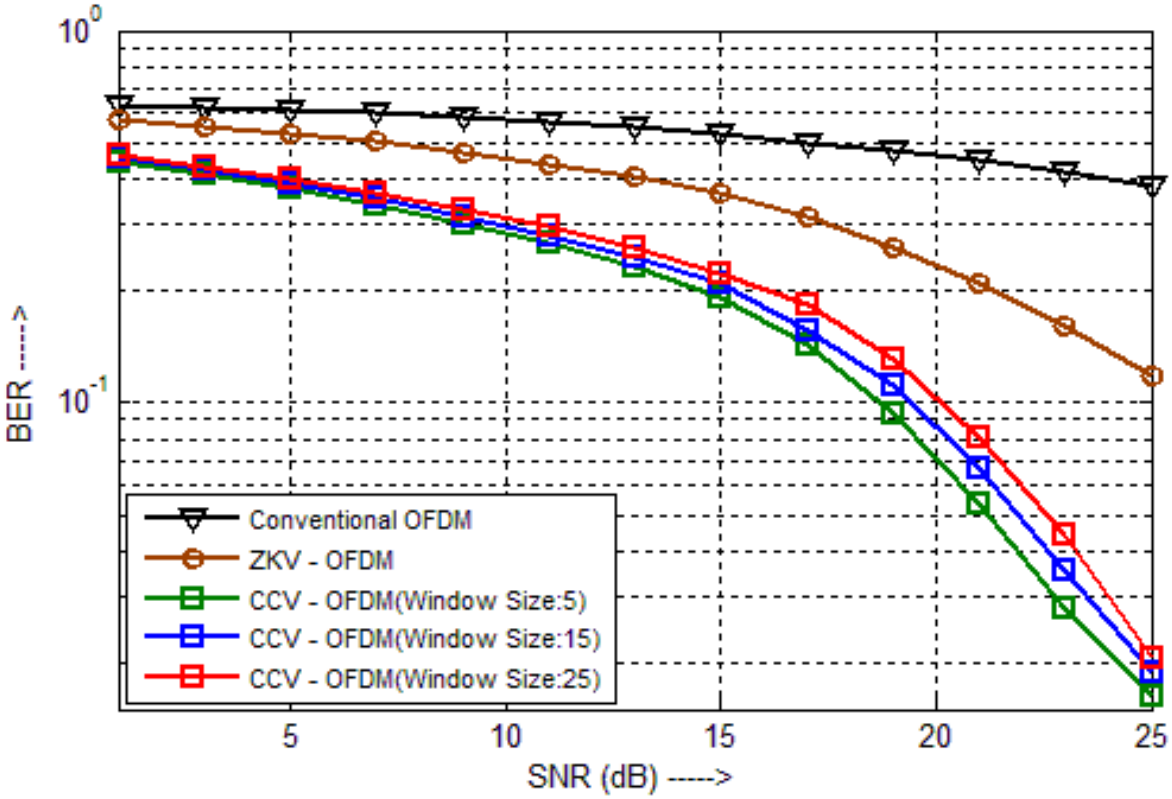

Fig.5.17. BER vs. SNR (dB) for different window size for CCV- method with 1024 subcarriers.

5.4.2 Performance of OFDM System with Mitigation Methods Under Imperfect CSI

- **Case 1: Comparison of the Three Underlying Systems with Channel Estimation Error**

In this simulation, we compare the BER performance of conventional OFDM, ZKV-OFDM and CCV-OFDM using imperfect CSI for symbol detection. The value of H_{avg} is 0.75, number of impulses is kept 10% in a symbol duration at 20dB SNR, $C = 0.25$ in ZKV-OFDM, window size is 15 in CCV-OFDM, and the modulation used is 16-QAM. The simulation results illustrated in Fig. 5.18 show that CCV-OFDM outperforms ZKV-OFDM and conventional OFDM in case of the usage of imperfect CSI at low and moderate channel estimation error values. However under high channel estimation error scenario, the BER performance of all three methods gets substantially degraded.

Table 5.6. System parameters for simulation under imperfect CSI.

Parameter	**Value**
Modulation used	16-QAM
Number of subcarriers	256
Number of impulses	10% of the symbol period, N
Average value for a single channel-tap coefficient $\left(H_{avg}\right)$	0.75
Parameter C for ZKV method	0.25
Window Size for CCV method	15
SNR	20 dB

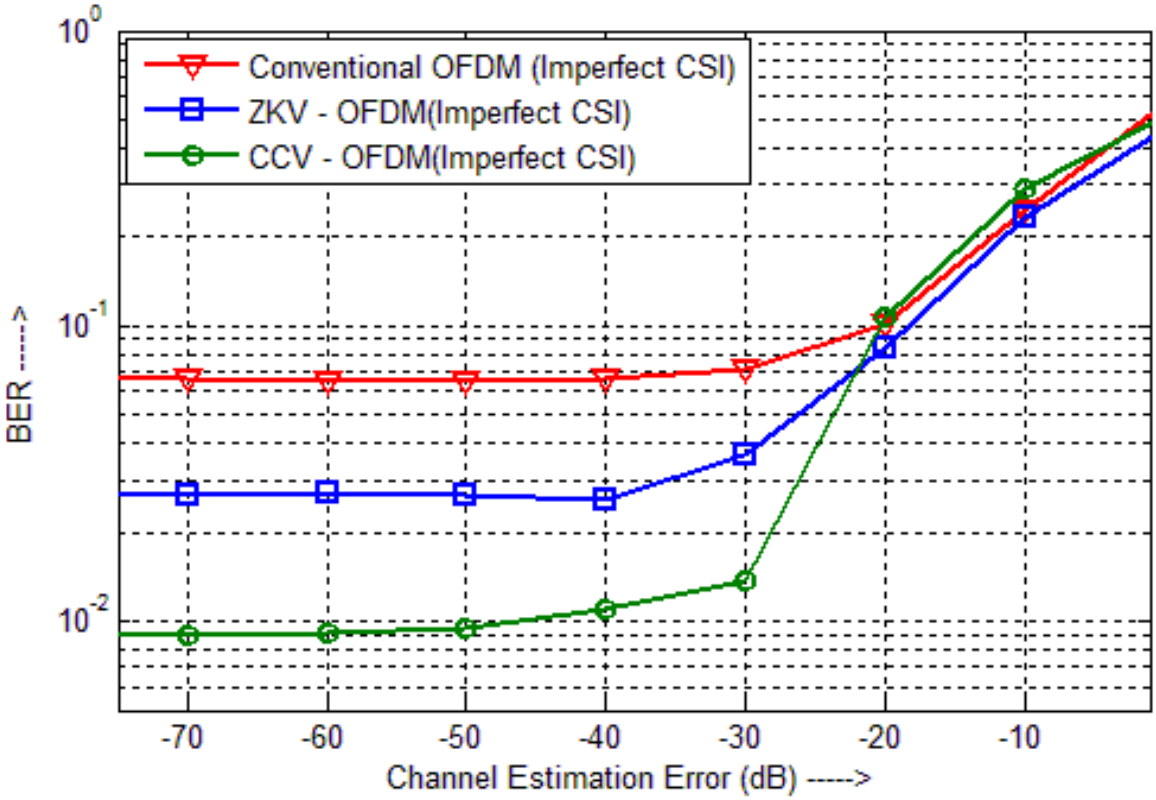

Fig. 5.18. BER vs. channel estimation error (dB) under impulsive environment.

- **Case 2: Analysis with Different Modulation Schemes**

We next compare the performance of ZKV-OFDM and CCV-OFDM using different modulation techniques i.e., QPSK, 16-QAM and 64-QAM. All the parameter settings are kept same as in the above case, but SNR is fixed at 15dB. It is clear from results showcased in Fig. 5.19 that for 64-QAM, the performance of ZKV-OFDM and CCV-OFDM is inferior to QPSK modulation technique because distance between constellation points decreases for 64-QAM if we keep the total transmitted power constant. Therefore, the symbol errors are more in case of 64-QAM system. Although QPSK modulation is giving better BER results, yet the comparative data rate is less.

Table 5.7. System parameters for simulation for different modulation schemes under imperfect CSI.

Parameter	**Value**
Modulation used	QPSK, 16-QAM, 64-QAM
Number of subcarriers	256
Number of impulses	10% of the symbol period, N
Average value for a single channel-tap coefficient $\left(H_{avg}\right)$	0.75
Parameter C for ZKV method	0.25
Window Size for CCV method	15
SNR	15 dB

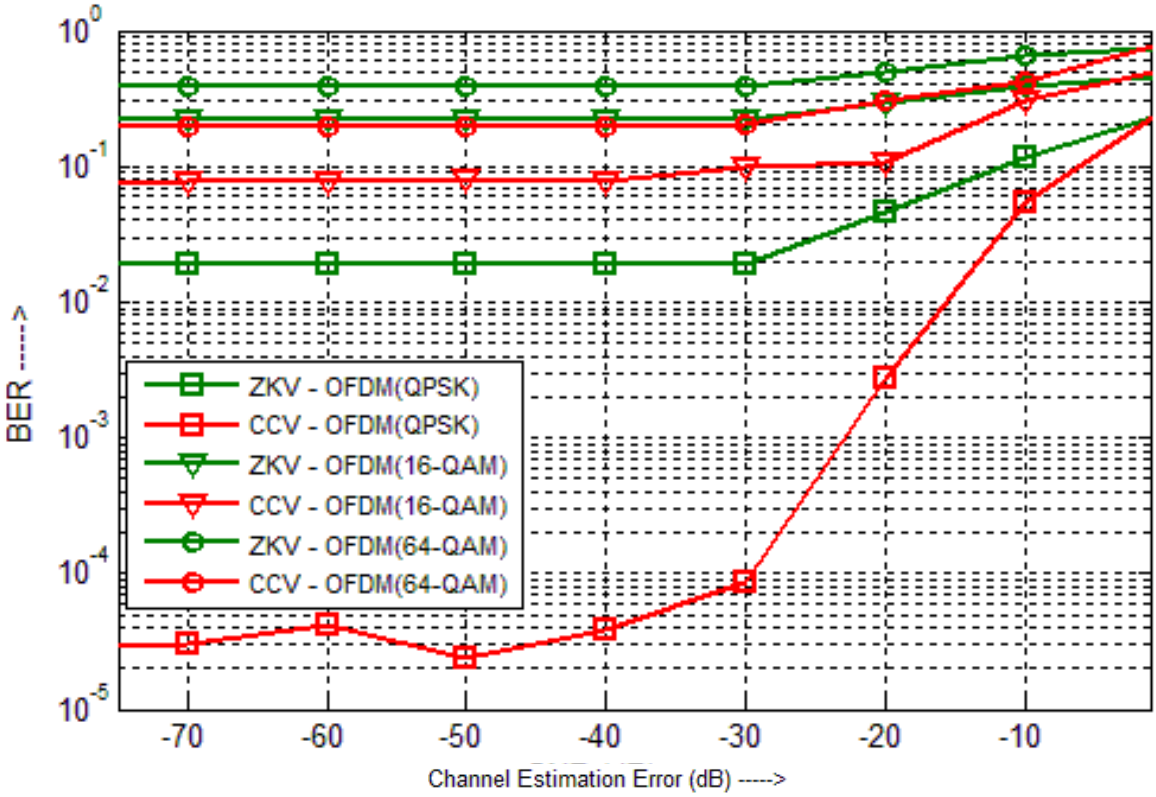

Fig. 5.19. BER vs. channel estimation error (dB) for different modulation schemes.

- **Case 3: Analysis with Different Number of Impulses**

Subsequently, we observe the impact of the number of impulses on BER performance of ZKV-OFDM and CCV-OFDM at $-40\,dB$ channel estimation error variance. For this, the number impulses are considered to be 15% and then reduced to 5% in one symbol period for 16-QAM. The value of H_{avg} is 0.75, C is 0.25 for ZKV-OFDM and window size is 15 for CCV-OFDM. It is observed from simulation results in Fig. 6 that CCV-OFDM outperforms ZKV-OFDM in the presence of impulsive noise. At $BER = 0.1$, CCV-OFDM system gives performance advantage of approximately 7dB over the ZKV-OFDM system. As the number of impulses decreases from 15% to 5% in a symbol duration, the performance of CCV-OFDM system gets improved by approximately 2 dB in terms of SNR at $BER = 0.01$, but this advantage is approximately 1dB in the case of ZKV-OFDM system. Therefore, CCV-OFDM system has an edge over ZKV-OFDM system using imperfect CSI under the fading environment in case of impulsive noise.

Table 5.8. System parameters for different number of noise impulses under imperfect CSI.

Parameter	**Value**
Modulation used	16-QAM
Number of subcarriers	256
Number of impulses	5%, 15% of the symbol period, N
Average value for a single channel-tap coefficient $\left(H_{avg}\right)$	0.75
Parameter C for ZKV method	0.25
Window Size for CCV method	15
Channel Estimation Error	-40 dB

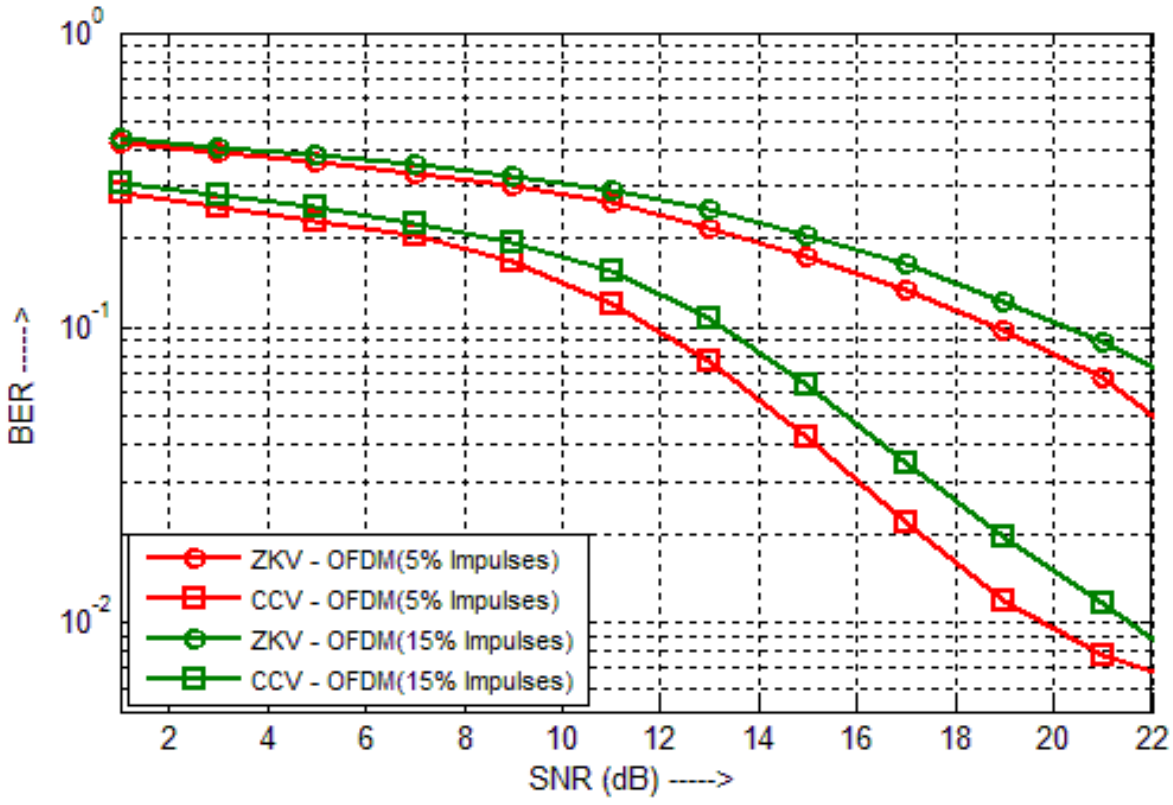

Fig. 5.20. BER vs. SNR (dB) for different number of noise impulses.

Chapter 6

CONCLUDING REMARKS AND FUTURE SCOPE

6.1 Concluding Remarks

This research work presents the optimization of the parameters used in ZKV method, proposed by Zhidkov, in [14], and CCV method, proposed by Jia and Meng, in [15], working under different fading conditions for perfect CSI as well as imperfect CSI in impulsive environment. For the many applications of OFDM system, mainly in the urban environment, impulsive noise is one of the main factors contributing to a significant reduction in the BER and/or symbol-error-rate (SER) performance. Hence, mitigating impulsive noise, in such corrupted environments, is one of the main factors considered in designing the system. It can be observed from the literature survey that many different schemes have been proposed and each one has its own advantageous side, effectiveness and limitations. This research work analyses, compares and optimizes two methods that effectively estimate and suppress the impulsive noise from the received signal in the frequency-domain. These methods provide significant advantage over conventional OFDM system that does not employ any impulsive noise mitigation scheme. While optimizing the parameters used in these methods the performance has improved further.

When working under perfect CSI environment, the parameter C of the ZKV scheme has been optimized. It has been observed by heuristic simulations that for $C = 0.25$, ZKV system has the best performance but CCV scheme still supersedes it. The window size for the CCV scheme has also been optimized and for window size of 5, best BER performance has been observed. The three OFDM systems: conventional OFDM, ZKV-OFDM system and CCV-OFDM system, are also analysed for different modulation schemes, different number of noise impulse pulses and different fading conditions. The performance of these systems is highly dependent on these conditions and significant variations have been observed while going from one parameter to another in the simulation. For the case of perfect CSI, CCV method has outperformed the ZKV method under all the conditions studied.

The channel estimation process cannot be perfect even when using linear or nonlinear adaptive filters. The inevitable error introduced in the estimation process also affects the performance of the underlying system. Hence, the three systems are further analysed for imperfect CSI. CCV-OFDM system has the best performance under imperfect CSI followed

by ZKV-OFDM system; and the conventional OFDM system has the worst performance. The ZKV-OFDM system and CCV-OFDM system are further analysed by varying the modulation schemes and the number of noise impulse pulses. As the order of the modulation scheme is decreased, the BER performance of both the system shows great improvement at the cost of decreased data rate. In all the three modulation schemes that are analysed in this research paper, CCV-OFDM system outperforms ZKV-OFDM system even in the case of imperfect CSI. When the number of impulses decreases from 15% to 5%, both the systems shows advantages in their performance. Even under highly corrupted impulsive environment, it has been observed that CCV scheme is a better impulsive noise suppression technique.

6.2 Future Scope

- Adaptive modulation schemes can be used for better BER performance with higher data rates. These schemes can be implemented for perfect CSI and imperfect CSI under different fading conditions [50].
- CCV scheme has proven to be a better option for impulsive noise suppression, but it has high computational complexity as compared to ZKV scheme. This would, hence, require more silicon area. Complexity reduction of such schemes can be the future scope.
- Different channel estimation schemes can be used for analysing the performance of OFDM system for imperfect CSI [49].

REFERENCES

[1] R. Prasad, *OFDM for Wireless Communication*, 2nd ed. Artech House, UK: Universal Personal Communications, 2004.

[2] H. Liu and G. Li, *OFDM based Broadband Wireless Networks: Design and Optimization*, 1st ed. Hoboken, NJ: John Willey & Sons, 2005.

[3] Y. Li, L. J. Cimni, and N. R. Sollenberger, "Robust channel estimation for OFDM systems with rapid dispersive fading channels," *IEEE Trans. on Commun.*, vol. 46, no. 7, pp. 902-915, July 1998.

[4] J. Armstrong, "OFDM for optical communications," *J. of Lightw. Technol.*, vol. 27, no. 3, pp. 189-204, February 2009.

[5] C. H. Yih, "Iterative interference cancellation for OFDM signals with blanking nonlinearity in impulsive noise channels," *IEEE Signal Process. Lett.*, vol. 19, no. 3, pp. 147-150, March 2012.

[6] M. G. Sanchez, L. de Haro, M. C. Ramon, A. Mansilla, C. M. Ortega, and D. Oliver, "Impulsive noise measurements and characterization in a UHF digital TV channel," *IEEE Trans. on Electromagnetic Compatibility*, vol. 41, no. 2, pp. 124-136, May 1999.

[7] I. Mann, S. McLaughlin, and W. Henkel, "Impulse Generation with appropriate amplitude, length, inter-arrival, and spectral characteristics," *IEEE J. on Select. Areas Commun.*, vol. 20, no. 5, pp. 901-912, August 2002.

[8] S. V. Zhidkov, "Performance analysis and optimization of OFDM receiver with blanking nonlinearity in impulsive noise environment," *IEEE Trans. on Veh. Technol.*, vol. 55, no. 1, pp. 234-242, January 2006.

[9] A. Mengi and A. Vinck, "Successive impulsive noise suppression in OFDM", in *Proc. IEEE Int. Symp. on Power Line Commun. Appl.*, Rio de Janerio, Brazil, March 2010, pp. 33-37.

[10] M. Ghosh, "Analysis of the effect of impulsive noise on multi-carrier and singlecarrier QAM systems," *IEEE Trans. on Commun.*, vol. 44, no. 2, pp. 145-147, February 1996.

[11] H. A. Suraweera, C. Chai, J. Shentu, and J. Armstrong, "Analysis of impulse noise mitigation techniques for digital television systems," in *Proc. 8th Int. OFDM Workshop*, Hamburg, Germany, September 2003, pp. 172-176.

[12] H. A. Suraweera and J. Armstrong, "Noise bucket effect for impulsive noise in OFDM," *IET Electron. Lett.*, vol. 40, no. 8, pp. 1156-1157, September 2004.

[13] J. Armstrong and H. A. Suraweera, "Impulsive noise mitigation for OFDM using decision directed noise estimation," *IEEE Int. Symp. on Spread Spectrum Techniques and Applicat.*, pp. 174-178, September 2004.

[14] S. V. Zhidkov, "Impulsive noise suppression in OFDM based communication system," *IEEE Trans. on Consum. Electron.*, vol. 49, no. 4, pp. 944-948, November 2003.

[15] J. Jia and J. Meng, "A dual protection scheme for impulsive noise suppression in OFDM systems," *Int. J. Electron. and Commun. (AEÜ)*, vol. 68, no. 1, pp. 51–58, January 2014.

[16] A. Bansal and A. K. Kohli, "Suppression of impulsive noise in OFDM system using imperfect channel state information," *Elsevier, Optik—Int. J. Light Electron Optics*, vol. 127, no. 4, pp. 2111–2115, February 2016.

[17] F. Abdelkefi, P. Duhamel, and F. Alberge, "Impulsive noise cancellation in multicarrier transmission," *IEEE Trans. on Commun.*, vol. 53, no. 1, pp. 94-106, January 2005.

[18] T. Y. Al-Naffouri, A. K. Narayanan, and G. Caire, "Impulse noise cancellation in OFDM: an application of compressed sensing," *IEEE Int. Symp. on Inf. Theory*, Toronto, pp. 1293-1297, July 2008.

[19] Y. Chen, J. Zhang, and A. D. S. Jayalath "Estimation and compensation of clipping noise in OFDMA systems," *IEEE Trans. on Wireless Commun.*, vol. 9, no. 2, pp. 523-527, July 2010.

[20] T. Kitamura, K. Ohno, and M. Itami, "Iterative impulsive noise reduction by generating its replica signal in OFDM reception," *IEEE Int. Conf. on Consum. Electron.*, Las Vegas, pp. 389-390, January 2011.

[21] L. Lampe, "Bursty impulse noise detection by compressed sensing," *IEEE Int. Symp. on Power Line Commun.*, Udine, pp. 30-34, April 2011.

[22] T. Y. Al-Naffouri, A. A. Quadeer, and G. Caire, "Impulsive noise estimation and cancellation in DSL using orthogonal Clustering," *IEEE Int. Symp. on Inf. Theory*, Toronto, pp. 2841-2845, August 2011.

[23] D. Tseng, Y. S. Han, W. H. Mow, L. Chang, and A.J. Han Vinck, “Robust clipping for OFDM transmissions over memory-less impulsive noise channels,” *IEEE Commun. Lett.*, vol. 16, no. 7, pp. 1110-1113, July 2012.

[24] G. Ren, S. Qiao, H. Zhao, C. Li, and Y. Hei, “Mitigation of periodic impulsive noise in OFDM-based power-line communications,” *IEEE Trans. on Power Del.*, vol. 28, no. 2, pp. 825-834, April 2013.

[25] M. E. Mathew and J. Jeevitha, “An impulsive noise cancellation using iterative algorithms,” *IEEE Int. Conf. on Electron. and Commun. Syst.*, Coimbatore, pp. 1-6, February 2014.

[26] Y. Wu and W. Y. Zou, “Orthogonal frequency division multiplexing: A multicarrier modulation scheme,” *IEEE Trans. on Consum. Electron.*, vol. 41, no. 3, pp. 392-399, August 1995.

[27] L. L. Hanzo, M. Munster, B. J. Choi, T. Keller, *OFDM and MC-CDMA for broadband multi-user communications, WLANs and Broadcasting*, 1st ed., Chichester, UK, Wiley-IEEE Press, 2003.

[28] J. G. Prokias, *Digital Communications*, 5th ed. Avenue of the America, NY: McGraw-Hill, 2008.

[29] S. B. Wienstein and P. M. Ebert, “Data transmission by frequency-division multiplexing using discrete Fourier transform,” *IEEE Trans. on Commun. Tech.*, vol. 19, no. 5, pp. 628-634, October 1971.

[30] S. B. Bulumulla, S. A. Kassam, and S. S. Venkatesh, “A systematic approach to detecting OFDM signals in a fading channel,” *IEEE Trans. on Commun.*, vol. 48, no. 5, pp. 725-728, May 2000.

[31] Y. H. Ma and E. Gunawan, “Performance analysis of the OFDM system for broadband power line communications under impulsive noise and multipath effects,” *IEEE Trans. on Power Del.*, vol. 20, no. 2, pp. 674-682, April 2005.

[32] Y. Zhao and S. Haggman, “Inter-carrier interference self-cancellation scheme for OFDM mobile communication systems,” *IEEE Trans. on Commun.*, vol. 49, no. 7, pp. 1185-1191, July 2001.

[33] Y. Li, “Pilot-symbol-aided channel estimation for OFDM in wireless systems,” *IEEE Trans. veh. Technol.*, vol. 49, no. 4, pp. 1207-1215, July 2000.

[34] O. Gonzalez, R. Perez-Jimenez, S. Rodriguez, J. Rabadan, and A. Ayala, “OFDM over indoor wireless optical channel,” *IEEE Proc. Optoelectron.*, vol. 152, no. 4, pp. 199-204, March 2006.

[35] T. M. Schmidl and D. C. Cox, "Robust frequency and timing synchronization for OFDM," *IEEE Trans. on Commun.*, vol. 45, no. 12, pp. 1613-1621, December 1997.

[36] N. A. Gugudu, "Evaluation of channel coding in OFDM systems," M. Tech thesis, Dept. Electron. and Commun. Eng., National Institute of Technology, Rourkela, 2006.

[37] A. Pavani, E. V. K. Rao, and B. P. Rao, "A new OFDM standard for high rate wireless LAN in the 5 GHZ band," *Int. J. of Future Gen. Commun. and Netw.*, vol. 4, no. 4, pp. 57-64, December 2011.

[38] K. Fazel, "Performance of OFDM for mobile communication system," *IEEE Pers. Commun.*, vol. 2, pp. 975-979, October 1993.

[39] B. Sklar, *Digital Communications: Fundamentals and Applications*, 2nd ed., Upper Saddle River, NJ: Prentice Hall, 2002.

[40] Y. Mostofi and D. C. Cox, "Mathematical analysis of the impact of timing synchronization errors on the performance of an OFDM system," *IEEE Trans. Commun.*, vol. 54, no. 2, pp. 226-230, February 2006.

[41] L. Wan and V. K. Dubey, "Bit error probability of OFDM system over frequency nonselective fast Rayleigh fading channels," *IEEE Electron. Lett.*, vol. 36, no. 15, pp. 1306-1307, July 2000.

[42] A. Goldsmith, *Wireless Communication*, 2nd ed., West 20th Street, NY: Cambridge University Press, 2005.

[43] T. S. Rappaport, *Wireless Communications*, 3rd ed., Upper Saddle River, NJ: Prentice Hall, 1996.

[44] S. V. Vaseghi, *Advance Digital Signal Processing and Noise Reduction*, 2nd ed., West Sussex, UK: John Wiley & Sons, 2008.

[45] K. L. Blackard, T. S. Rappaport, and C. W. Bostian, "Measurement and models of radio frequency impulsive noise for indoor wireless communications," *IEEE J. Sel. Areas Commun.*, vol. 11, no. 7, pp. 991-1001, September 1993.

[46] D. Middleton, "Statistical-physical models of electromagnetic interference," *IEEE Trans. Electromagn. Compat.*, vol. 19, no. 3, pp. 106-127, August 1977.

[47] A. Leke and John M. Cioffi, "Impact of imperfect channel knowledge on the performance of multi-carrier systems," *IEEE Conf. on Global Telecommun.*, Sydney, vol. 2, pp. 951-955, November 1998.

[48] A. Rai and A. K. Kohli, "Adaptive polynomial filtering using generalized variable step-size least mean pth power (LMP) algorithm," *Springer, Circuits Syst. Signal Process.*, vol. 32, no. 12, pp. 3931-3947, May 2014.

[49] A. K. Kohli and D. S. Kapoor, “Adaptive filtering techniques using cyclic prefix in OFDM systems for multipath fading channel prediction,” *Springer, Circuits Syst. Signal Process.*, Published online, pp. 1-24, December 2015.

[50] A. K. Kohli, “Fading model for antenna array receiver for a ring-type cluster of scatterers,” *Taylor & Francis Int. J. Electron.*, vol. 98, no. 7, pp. 933 – 940, July 2011.

LIST OF PUBLICATIONS

[1] S. Sehrawat and A. K. Kohli, "Suppression of impulsive noise in OFDM system using imperfect channel state information," *Elsevier, Optik—Int. J. Light Electron Optics,* Under Review, 2016.

801463026

by Shivani Sehrawat

FILE	SHIVANISEHRAWAT_801463026.PDF (1.62M)		
TIME SUBMITTED	30-JUN-2016 08:44PM	WORD COUNT	17171
SUBMISSION ID	687237273	CHARACTER COUNT	88845

801463026

ORIGINALITY REPORT

19%	8%	14%	10%
SIMILARITY INDEX	INTERNET SOURCES	PUBLICATIONS	STUDENT PAPERS

PRIMARY SOURCES

1	Submitted to Thapar University, Patiala Student Paper	4%
2	www.ukessays.com Internet Source	1%
3	Armstrong, Jean. "OFDM for Optical Communications", Journal of Lightwave Technology, 2009. Publication	1%
4	Yan Yao. "Performance improvement of V-BLAST after an initial estimate", VTC-2005-Fall 2005 IEEE 62nd Vehicular Technology Conference 2005, 2005 Publication	1%
5	Sunghyun Choi. "Multipath Channels", Wiley Encyclopedia of Electrical and Electronics Engineering, 12/27/1999 Publication	1%
6	Bansal, Abhishek, and Amit Kumar Kohli. "Suppression of impulsive noise in OFDM system using imperfect channel state information", Optik - International Journal for Light and Electron Optics, 2016.	1%